ORIGINAL PAPER

Geochemical controlling mechanisms and quality of the groundwater resources in El Fayoum Depression, Egypt

Mohamed Gad [1] (iD) · Maged El Osta [2,3]

Abstract
The main groundwater aquifer in El Fayoum region is a Quaternary aquifer. It shows increasing signs of groundwater quality deterioration. Therefore, a comprehensive assessment of groundwater quality has been performed for determining the geochemical processes affecting the groundwater quality evolution and assessing groundwater quality for drinking and irrigation uses. Physicochemical parameters, geochemical model (NETPATH), and water quality indices (WQIs) are applied to improve water quality assessment and controlling mechanisms with help of statistical analysis and GIS techniques. Thirty-eight groundwater samples from the Quaternary aquifer at depths less than 60 m and 12 irrigation drainage samples were collected. Thirteen physicochemical parameters including temperature (°C), TDS, pH, EC, K^+, Na^+, Ca^{+2}, Mg^{2+}, HCO_3^-, Cl^-, SO_4^{2-}, CO_3^{2-}, and NO_3^- were measured by standard analytical techniques. The analytical findings reveal that the groundwater facies are Na-Cl, mixed Ca-Mg-Cl, and Na-Ca-HCO$_3$ water types. In addition, the minerals saturation indices (SI) estimated by a geochemical model revealed that the groundwater samples are supersaturated by kaolinite, Ca-montmorillonite, dolomite, gibbsite, calcite, quartz, and aragonite and are unsaturated by gypsum, anhydrite, and partial pressure of CO_2. The drinking water quality index (DWQI) results revealed that 58% of the groundwater samples are very poor quality, while 42% of samples are unsuitable for drinking uses. The irrigation water quality index (IWQI) results revealed that all groundwater samples range from 26.1 to 36.1, indicating a medium class of quality for irrigation purposes. These results reflect the influences of the high mineralization processes, cumulative effect of cation exchange, leaching processes from aquifer materials, contamination by irrigation return flow, and seepage from drains on the groundwater quality. In conclusion, utilization of physicochemical parameters, geochemical model, and WQIs can be considered as a promising and applicable approach to determine the controlling geochemical mechanisms and for assessing of groundwater quality in El Fayoum Depression, Egypt.

Keywords Physicochemical data · NETPATH model · Water quality indices · El Fayoum Depression · Egypt

✉ Mohamed Gad
  mohamed.gad@esri.usc.edu.eg

[1] Evaluation of Natural Resources Department, Environmental Studies and Research Institute (ESRI), University of Sadat City, Sadat City, Minufiya 32897, Egypt

[2] Water Research Center, King Abdulaziz University, Jeddah, Saudi Arabia

[3] Geology Deparment, Faculty of Science, Damanhour University, Damanhour 22511, Egypt

Introduction

The growing population has led to increasing demand for groundwater for drinking and irrigation usages. Hydrological and geochemical conditions represented in aquifer characteristics and geochemical processes control the groundwater quality. Recently, assessment of groundwater quality for drinking and irrigation usages in developing countries is important, since water quality is a fundamental aspect of groundwater management (Li et al. 2018; Wu et al. 2019). In addition, it identified the geochemical mechanisms affecting on the water chemistry (Ndoye et al. 2018; Subba Rao and Chaudhary 2019). The geochemical characteristics of groundwater depend mainly on recharge, aquifer materials, residence time, and some geochemical reactions such as leaching, mineral dissolution, and ion exchange. However, water quality

management should be determined through comprehensive groundwater quality assessment and physicochemical characteristics of the groundwater. The quality of water is a function of its physicochemical parameters that reflect groundwater characteristics and factors controlling the quality of water (Joshi and Seth 2011; Hussein et al. 2017; Egbueri 2018; Zhang et al. 2018; Mgbenu and Egbueri 2019).

Therefore, the imitative techniques such as Piper trilinear diagram (Piper 1944), Chadah diagram (Chadha 1999), Gibbs diagram (Gibbs 1970), and hydrochemical facies evolution diagram (HFE) (Giménez-Forcada and San Román 2015) are applicable and widely used techniques for identifying the major geochemical processes that control the water evolution (Kumar et al. 2015), which were used to evaluate water quality and their controlling mechanisms in this study.

Correlation matrix (CM) is powerful tool to identify significant physicochemical parameters and the interrelations between these parameters to understand the main factors influencing the distribution of these parameters in groundwater resources (Singaraja et al. 2015; Kumar et al. 2018; Li et al. 2019b).

In addition, a geochemical modeling (NETPATH) is a significant method to assess groundwater quality and understand the main geochemical characteristics influencing groundwater quality. The minerals saturation index (SI) reflect the geochemical reactions; including rock-water interaction, dissolution reactions, solubility of salts, precipitation, evapotranspiration, ion exchange, and the anthropogenic activities; which depend on the groundwater physicochemical characters and the aquifer matrix (Bozdag and Goçmez 2013; Gad and Saad 2017; Khan et al. 2017; Gad et al. 2018; Li et al. 2019a).

In a groundwater system, the inverse method can be used according to a geochemical model to simulate the net geochemical mass balance transfer and reactions of possible minerals and gases. This model helps to calculate the amounts of chemical constituents in groundwater that are generated from the dissolution or precipitation of main mineral phases (El Osta et al. 2020).

In general, contamination by trace elements associated with farming affects not only human health but also plants, due to their toxic effects, especially in developing countries. The extensive use of fertilizers and pesticides in land reclamation areas leads to degradation of the groundwater quality, especially in the shallow groundwater aquifers (Bartzas et al. 2015; Dhanasekarapandian et al. 2016; Sharma et al. 2020).

Therefore, the physicochemical data and WQIs present a useful interpretation of groundwater quality for irrigation and drinking uses (Bora and Goswami 2017). The drinking water quality index (DWQI) is a powerful approach to reveal the cumulative influences of different physicochemical parameters, according to the weight and rate of each parameter, and express groundwater quality (Rana et al. 2018). Each physicochemical parameter has a weight based on its relative effect

on the groundwater quality for drinking use (Chaurasia et al. 2018). The irrigation water quality index (IWQI) combines the effects of five hazard groups, which are integrated together to give a single value that reflects the quality of the groundwater for irrigation use (Chukwuma et al. 2016). These hazard groups are the permeability hazard, salinity hazard, specific ion toxicity, and miscellaneous hazards, according to the guidelines of Ayers and Westcot (1994). In addition, sodium absorption ratio (SAR) is an important index for determining the suitability of water for irrigation with respect to sodium hazard (Richards 1954), since it is more closely related to exchangeable sodium percentage in the soil (Tiwari and Manzoor 1988).

The main groundwater resource in El Fayoum Depression is a Quaternary aquifer, and it shows increasing signs of groundwater quality deterioration according to previous works (Abdel Kawy and Belal 2012; Gad and El-Zeiny 2016; Gad and El-Hattab 2019), which might be attributed to irrigation return flow and anthropogenic activities.

Groundwater chemistry focused on hydrochemical criteria provides preliminary information on water types, various geochemical processes, and water classification for drinking and irrigation usages. Therefore, the objectives of this work were (i) to investigate groundwater types, and geochemical facies evolution based on hydrogeological conditions and physicochemical parameters of the groundwater resources; (ii) to identify the geochemical controlling mechanisms affecting on water chemistry with help of a geochemical modeling; and (iii) to assess the suitability of the groundwater for drinking and irrigation purposes using WQIs.

The integration of physicochemical parameters, geochemical modeling, and WQIs with help of statistical analysis and GIS techniques provides a valuable framework for assessing patterns, defining particular environmental problems, and sharing knowledge on water resources, geochemical processes, and water quality.

Study area

El Fayoum Depression is a green, fertile area that is considered one of the most important agriculture sectors in Egypt, represents more than 5% of the total cultivated area of Egypt which, contributing about 20.54% to the country's gross domestic product (El Sheikh 2004; Ahmed 2012). The main crops cultivated in the investigated area are wheat, cotton, maize, sunflower, clovers, tomatoes, aromatic and medicinal plants, mangoes, olives, and citrus (Abd-Elmabod et al. 2019).

El Fayoum Depression is located at the semi-arid province in the western side of the Nile River. This depression lies between latitudes 29° 00′ and 29° 30′ N and longitudes 30° 20′ and 31° 10′ E, with an area of about 1200 km² (Fig. 1). The depression is bounded by Qarun Lake that has an area of about

Fig. 1 Location of the study area and measuring points
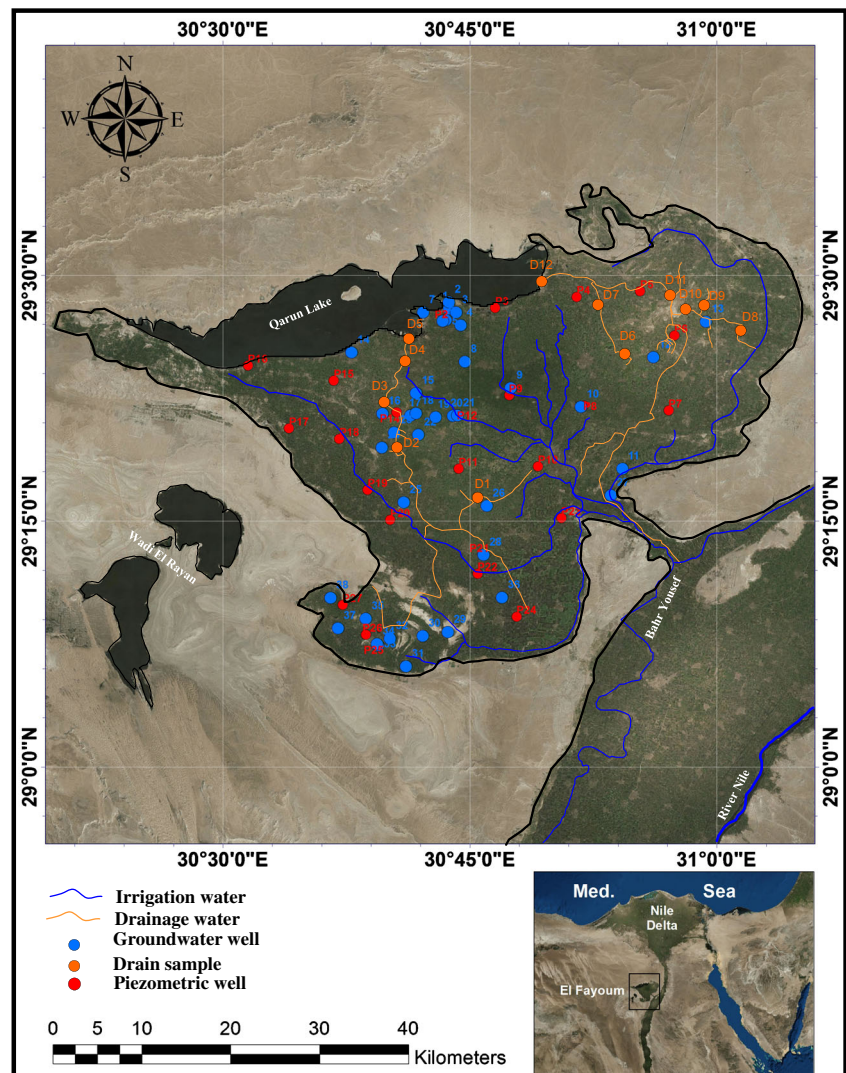
200 km^2 in the northwestern side and the Nile River in the southeastern side with an elevation varies from 37 m (amsl) at the southern part to about − 49 m (bmsl) in the north with a slope gradient downward from south to north ranges from 0 to 7 (Gad and El-Zeiny 2016; Gad and El-Hattab 2019). According to the meteorological data, the climate is generally dry and warm with a mean rainfall of 10 mm/year and a mean temperature and evaporation rate ranging from 14.5 to 31.0 °C, and from 0.0088 to 0.03 mm/year, respectively (Abdel Kawy and Belal 2012; Baioumy et al. 2010; Khalil et al. 2017).

Geology and hydrogeology

The lithological succession in El Fayoum Depression ranges from Quaternary to Tertiary (Fig. 2). El Fayoum Depression is mostly covered by Quaternary sediments which extend in the subsurface with variable thicknesses, which are mainly of fluvio-lacustrine origin. The Quaternary lacustrine deposits are dominating in the south of Qaroun Lake, which are consisting of clay stone, gypsum, and calcareous materials intercalated with ferruginous sandy silt (Redwan and Elhaddad 2017). The Quaternary sediments overlay the Middle Eocene deposits, which are composed of limestone, marl, sand, and gypferrous shale that cropped out surrounding the depression (Metwaly et al. 2010). The Middle Eocene deposits overlay the Oligocene deposits, which are composed of fluvio-marine variegated sands and sandstone, with alternating shale, marls, and calcareous beds. The sediments of Lower Miocene are composed of continental sandstone and conglomerate, while sediments of Pliocene are composed of calcareous sandstone and limestone. Several distortion lines, such as faults, breaks, and some folds striking N-S and NW-SE, that affect El Fayoum Depression are dominant at the peripheries of the depression (El-Sayed et al. 2015). Based on a detailed analysis of the available lithological data, two geological cross sections (N–S and SW–NE) were constructed (Fig. 3).
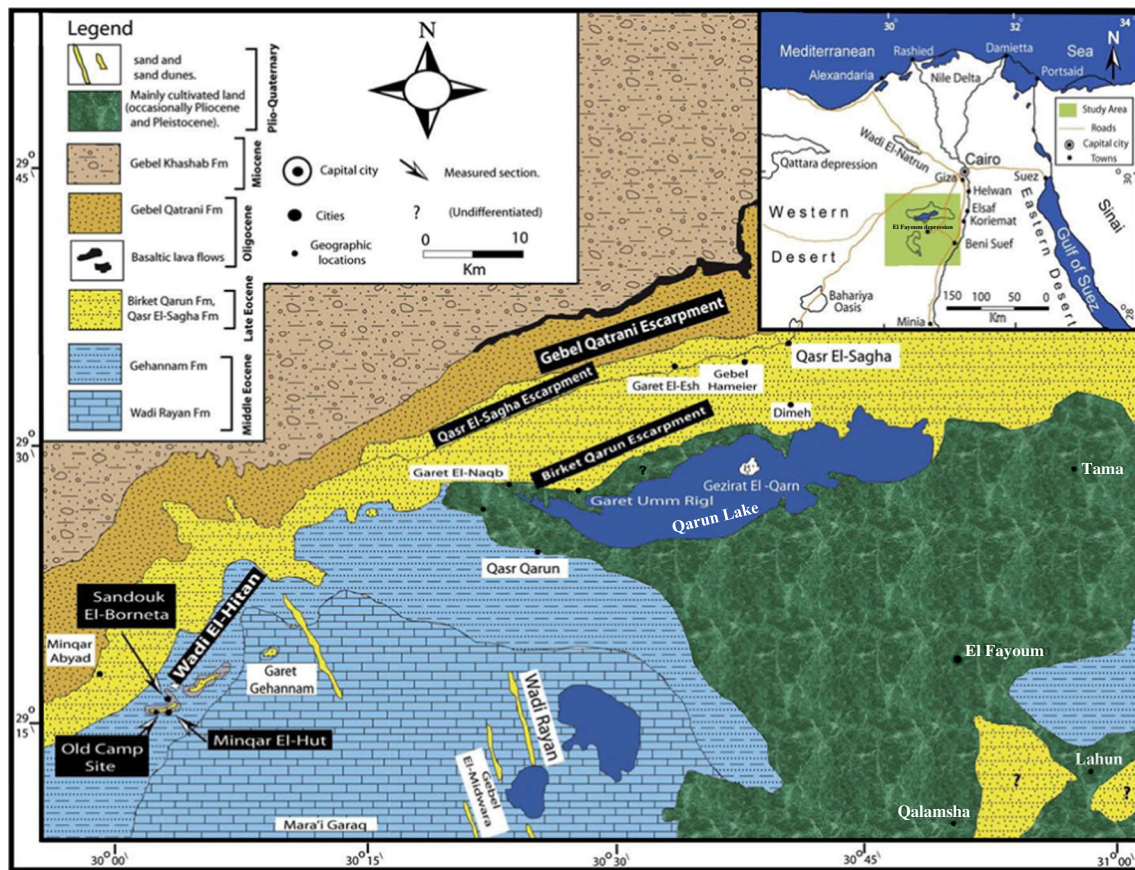
Fig. 2 Geological settings of El Fayoum Depression (Ahmed 2012)

The surface water system is represented by Nile River, irrigation canals, and drains. Bahr Youssef and Bahr Hassan Wassef canals deliver the Nile River water to the depression. Generally, three groundwater aquifers were distinguished in El Fayoum Depression (Mohamed et al. 2015) including Quaternary aquifer, Eocene aquifer, and Nubian sandstone aquifer. Quaternary aquifer is a perched aquifer that is maintained by infiltration from canals, drains, and irrigated fields. Beneath this aquifer, the Eocene aquifer, which is composed of limestone and marls, and it, has high salinity. The Nubian sandstone aquifer is a very deep aquifer (> 1000 m), and the depth to water is too great to allow exploitation at a dynamic level of + 25 m (amsl) where their waters are originated from the Nubian aquifer (El Sheikh 2004; Attia et al. 2018).

The Quaternary aquifer has its maximum thickness (about 60 m) at the center of the depression while, the minimum thickness is less than 1 m along the depression peripheries due to local faulting (Ahmed 2012). The groundwater depths varied from few centimeters to 9.1 m, with groundwater level ranges from + 20 m (amsl) in the area near Nile River to − 50 m (bmsl) near Qarun Lake (Fig. 4). In addition, the groundwater flows from SE to N and NW in concordance with the general slope of the depression topography (Gad and El-Hattab 2019). The Quaternary aquifer is thought to be recharged by the seepage from surface irrigation canals,

drains, and Nile River. In addition percolation from the underlying fractured limestone of the Eocene aquifer exists (El Sheikh 2004).

Material and methods

Sampling and analyses

Thirty-eight groundwater samples from shallow wells (< 60 m) and 12 samples from irrigation drainage canals were collected during summer 2018 in refined plastic bottles, and the sample bottles were rinsed with deionized water before sampling. Two groups of samples were collected from each sampling site, where the first group is used for major ions analyses. The second group was collected for heavy metals analyses and was acidified with nitric acid to a pH less than 2. All samples were preserved at temperature less than 4 °C until analyzing processes as required by standard procedures. Groundwater samples were bottled 0.45 mm polypropylene filter membranes, and then, the chemical analysis was performed using different apparatus and techniques. The physical parameters, temperature, pH, TDS, and EC, were immediately measured in the field using a portable calibrated salinity multi-parameter instrument (Hanna HI 9811-5).
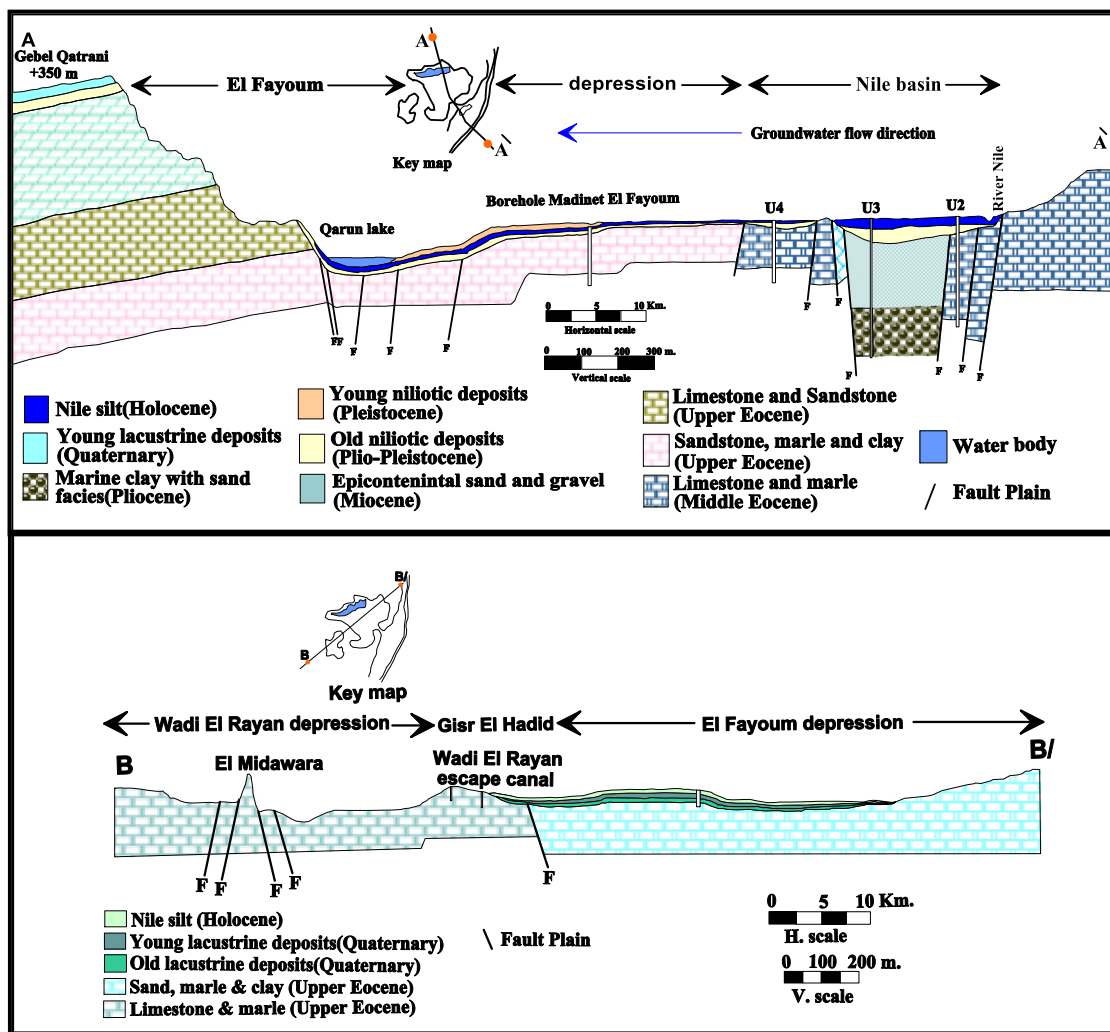
Fig. 3 Geological cross sections through El Fayoum Depression (Gad and El-Hattab 2019)

Major ions, Ca^{+2}, Mg^{2+}, Cl^-, HCO_3^-, and CO_3^{2-}, were analyzed by volumetric titration using a standard analytical method (APHA 2012). In addition, the ions of K^+ and Na^+ were analyzed using flame photometer (PFP7 U.K.). The UV/Visible spectrophotometer was used to analyze SO_4^{2-} and NO_3^-; in addition, silica (SiO_2) was analyzed using ion chromatography. The analytical results of the trace elements including Al, Ba, Cu, Cr, Cd, Mn, Fe, Ni, Pb, Sb, and Se that published in Gad and El-Hattab (2019) were taken into consideration in calculation of saturation index (SI) of minerals and WQIs. The mineralogical composition of the aquifer materials from the collected core samples was analyzed using Bruker X-Ray Diffractometer (XRD), D2 PHASER 2nd Gen.

## Data analysis and graphical approach

The groundwater data evaluation is carried out using statistical analysis (SPSS Inc., Chicago, IL, USA). The obtained analytical results were presented (Tables 1 and 2) and processed using ArcGIS version 10 to distribute the suitability of groundwater quality for drinking and irrigation usages. Hierarchical cluster analysis (HCA) was performed between groups linkage using SPSS with Euclidean distances as a measure of similarity to classify the similar water sampling sites according to the EC values.

A geochemical model, NETPATH software package v. 2.0 (Plummer et al. 1991), was applied for environmental simulation based on the physicochemical parameters of the collected groundwater samples to interpret the hydrochemistry of the groundwater resources depends on the equilibrium between mineral phases and water and is expressed by SI (Garrels and Christ 1965).

The imitative techniques including Piper diagram, Chadah diagram, Gibbs diagram, and HFE diagram were applied using Geochemist's Workbench Student Edition 12.0 software for identifying groundwater facies, geochemical processes, and the dominant groundwater chemistry control factors.

Fig. 4 Groundwater flow
directions in El Fayoum
Depression (Gad and El-Hattab
2019)
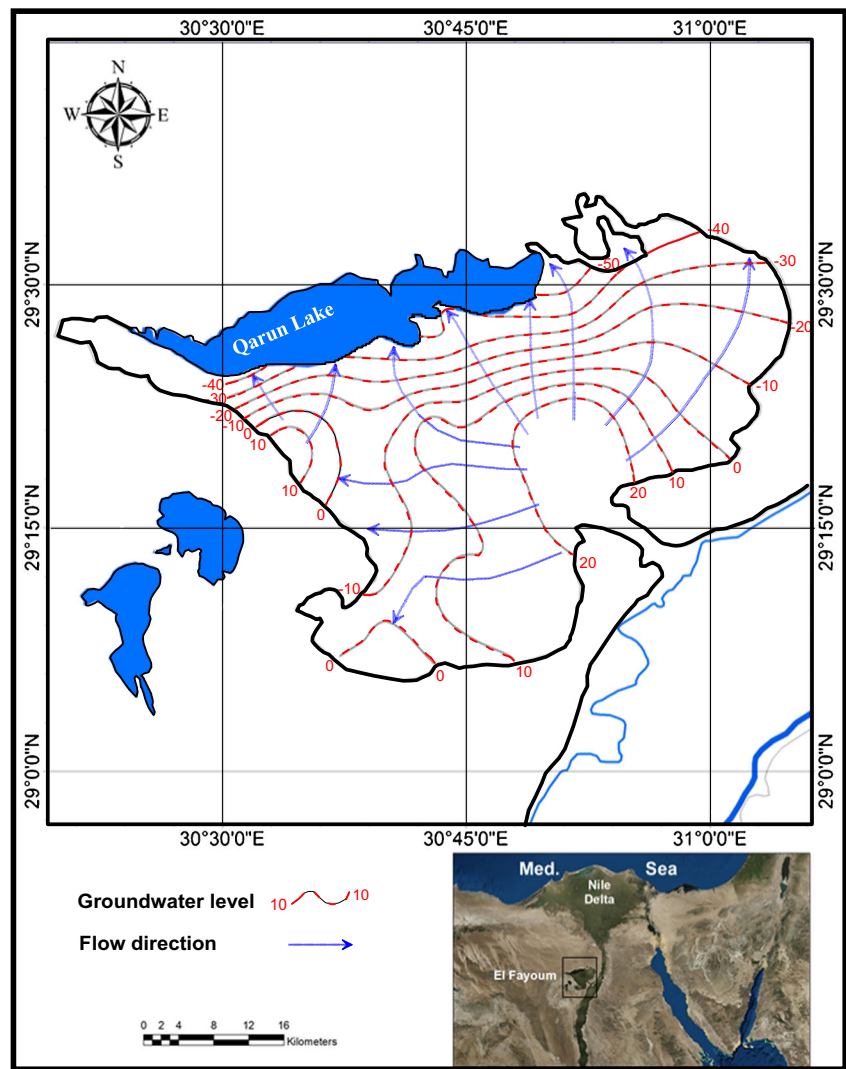
Table 1 Statistical description of the measured physicochemical parameters in the groundwater samples and irrigation drain canals

Parameter	T (°C)	pH	EC	TDS	Na$^+$	K$^+$	Mg^{2+}	Ca^{+2}	Cl$^-$	SO$_4^{2-}$	HCO$_3^-$	NO$_3^-$
Groundwater wells												
Min	27.00	6.40	959.84	614.30	110.00	6.00	24.00	46.40	85.00	51.60	72.00	3.500
Max	33.70	8.90	13,984.38	8950.00	2094.8	180.0	279.80	602.40	1992	3370.2	787.00	178.80
Mean	29.34	7.53	4315.33	2761.81	566.10	35.22	94.09	200.66	665.14	751.12	393.64	55.67
Stand. dev	1.77	0.56	3171.19	2029.56	505.61	39.38	49.86	144.90	504.21	829.04	137.60	47.16
Irrigation drainage canals												
Min	27.10	7.30	1017.00	651.00	89.80	8.46	22.20	52.40	116.24	26.91	128.00	15.14
Max	38.20	7.60	3546.00	2270.00	481.60	43.30	70.80	190.00	732.70	500.30	300.00	66.25
Mean	345.10	7.48	22,356.00	14,312.00	235.94	20.42	34.65	99.62	325.31	177.93	217.24	43.53
Stand. dev	28.76	0.11	1863.00	1192.67	123.87	10.63	15.87	51.15	205.25	128.33	57.11	16.45

All parameters are expressed in mg/L except T (°C), pH, and EC (μs/cm)

Table 2 Statistical description of minerals saturation index (SI) and PCO2

Minerals (SI)	Calcite	Aragonite	Dolomite	Gypsum	Anhydrite	Quartz	Gibbsite	Kaolinite	Ca-Mont.	PCO$_2$
Min	0.01	0.003	0.14	− 2.12	− 2.33	0.45	0.02	0.57	− 0.39	− 3.495
Max	1.9	1.76	3.9	− 0.03	− 0.23	0.90	1.84	5.84	5.23	− 0.738
Mean	0.69	0.59	1.45	− 1.01	− 1.21	0.68	0.83	3.68	2.85	− 2.023
Stand. dev	0.46	0.44	1.03	0.52	0.52	0.08	0.51	1.37	1.48	0.578

Indexing approach

Chloro-alkaline indices

The cation exchange reactions in groundwater resources were estimated through Chloro-alkaline indices (CAI I and CAI II) to assess the ion exchange reactions between groundwater and aquifer matrix according to Eqs. (1) and (2) that are expressed in mill equivalents per liter (Schoeller 1967).

$$CAI\ I = \frac{Cl^- - (Na^+ - K^+)}{Cl^-} \tag{1}$$

$$CAI\ II = \frac{Cl^- - (Na^+ - K^+)}{SO_4^{2-} + HCO_3^- + CO_3^{2-} + NO_3^-} \tag{2}$$

Mineral saturation indices

The saturation indices of the relevant minerals were estimated by simulating the net geochemical mass balance reactions to investigate thermodynamic influences on the composition of the groundwater (Ammar et al. 2014). The SI of particular minerals was estimated according to the following Eq. 3:

$$SI = Log\ (IAP/K_s) \tag{3}$$

where IAP is the ion activity product and K_s is the minerals solubility product.

The groundwater that is oversaturated for a mineral indicates SI is more than zero. Whereas SI is less than zero, indicates the sub-saturation state. The SI equals to zero indicates that a balance occurs between the minerals and groundwater. The SI of the collected groundwater samples was estimated using a net geochemical model, and the input data are the concentration of Na^+, Mg^{2+}, Ca^{+2}, Cl^-, SO_4^{2-}, HCO_3^-, CO_3^{2-}, NO_3^-, Al, Ba, Cu, Cr, Cd, Mn, Fe, Ni, Pb, Sb, and Se in mg/L as constrains, and the considered mineral phases in the geochemical model are H_4SiO_4, $CaCO_3$, $Mg(OH)_2$, $MgCO_3$, $MgSO_4$, SiO_2, $FeCl_2$, $FeSO_4$, $MnSO_4$, $AlOH_4$ and $AlSO_4$, according to the mineral composition of the shallow aquifer materials. The number of minerals is dependent on the input data, including available chemical variables (major cations and anions), metals, TDS, and pH at 25 °C.

Water quality indices

Water quality indices, DWQI, IWQI, and SAR, are important indices for demarcating the groundwater validity for drinking and irrigation usages.

Drinking water quality index

The groundwater evaluation for drinking purposes is identified by mathematical methods (DWQI), which is considered the useful index to measure the total quality of groundwater for drinking use (Kachroud et al. 2019). The DWQI is calculated using arithmetic weight method (Table 3), according to Eq. (4):

$$DWQI = \sum_{i=1}^{n} q_i W_i \tag{4}$$

where q_i is the sub quality index of each parameter, W_i is the weight unit of each parameter, and n is the number of parameters according to Eq. (5).

$$q_i = \frac{V_i - V_o}{S_i - V_o} \times 100 \tag{5}$$

V_i is a analyzed value of each parameter, S is the value of the standard permissible limit of each parameter, V_o is an the ideal value of each parameter, and V_o equals to zero for all parameters except for pH = 7.0 and DO = 14.6 mg/L (Tripaty and Sahu 2005).

W_i for each parameters is calculated according to the recommended standards (WHO 2017) by Eq. (6).

$$W_i = K/S_i \tag{6}$$

where K is the proportionality constant

Irrigation water quality index

The groundwater suitability for irrigation purposes is determined by IWQI (Table 5), which is the cumulative effect of five hazard groups (Simsek and Gunduz 2007) by Eq. (7).

$$IWQI = \sum_{i=1}^{5} G_i \tag{7}$$

Table 3 Calculation method of drinking water quality index (DWQI)

Parameter	Si (WHO 2017)	1/Si	Wi	qi
pH	8.5	0.117	0.000127	26.66
TDS	500	0.002	0.000002	166.2
EC	1500	0.0006	0.000001	86.56
TH	500	0.002	0.000002	65.94
K	12	0.083	0.000090	115.0
Na	200	0.005	0.000005	61.0
Mg	50.0	0.02	0.000022	73.4
Ca	75.0	0.013	0.000014	95.2
Cl	250	0.004	0.000004	54.84
SO_4	250	0.004	0.000004	78.08
HCO_3	120	0.008	0.000009	209.33
CO_3	350	0.0028	0.000003	0.00
NO_3	50.0	0.020	0.000022	7.00
Al	0.20	5.00	0.005412	6.05
As	0.00	100.0	0.108239	0.00
Ba	0.70	1.428	0.001546	11.4
Cd	0.003	333.33	0.360798	110
Cr	0.05	20.00	0.021648	9.60
Cu	2.00	0.500	0.000541	0.51
Fe	0.30	3.333	0.003608	10.93
Pb	0.01	100.0	0.108239	74.00
Mn	0.10	10.00	0.010824	6.3.00
Ni	0.02	50.00	0.054120	66.50
Sb	0.005	200.0	0.216479	42.00
Se	0.01	100.0	0.108239	176.0
		$k = [1/\sum(1/Sn)] = 0.00108$	$\sum wi = 1$	

where i is a cumulative index, G is the integration of 5 hazard components, and is calculated using Eq. (8).

$$G = \frac{w}{n}\sum_{k=1}^{n} r_k \qquad (8)$$

where:

$$G_1 = w_1 r_1 \qquad (9)$$

$$G_2 = w_2 r_2 \qquad (10)$$

$$G_3 = \frac{w_3}{3}\sum_{j=3}^{3} r_j \qquad (11)$$

$$G_4 = \frac{w_4}{N}\sum_{k=1}^{N} r_k \qquad (12)$$

$$G_5 = \frac{w_5}{3}\sum_{m=1}^{3} r_m \qquad (13)$$

where G_1 is the salinity hazard, G_2 is the infiltration and permeability hazard, G_3 is the specific ion toxicity, G_4 is the trace element toxicity, G_5 is the miscellaneous effects, w is the weight value of this group, r is the rating value of the parameter, k is a cumulative index, and n is the number of analyzed heavy metals.

Sodium absorption ratio

The SAR was estimated by a mathematical equation, which describes the water quality for irrigation usages according to Eq. (14), where all ions are expressed in meq/l (Richards 1954).

$$SAR = \left[Na^+ / \sqrt{\left(Ca^{2+} + Mg^{2+}/2\right)} \times 100 \right] \qquad (14)$$

Results

Physicochemical properties

The statistical description of physicochemical parameters in the collected groundwater samples revealed that pH values are ranged from 6.4 to 8.9, with a mean of 7.5. The groundwater pH values indicate that groundwater is slightly acidic. The temperatures of the groundwater varied from 29.7 to 30.2 °C depending on the groundwater depths (Fig. 4). The electrical conductivity (EC) values varied from 959.84 to 13984.37 μs/

cm, with a mean value of 4315.32 μs/cm. The values of TDS range from 614.3 to 8950 mg/L (Fig. 5), with a mean value of 2761.8 mg/L, where the groundwater quality belongs to brackish water type. The spatial distribution map of TDS was constructed as shown in Fig. 5. The salinity decreases toward the northeastern part of El Fayoum Depression and increases toward S, SW, NW, and WSW.

Sodium, K^+, Ca^{+2}, Mg^{+2}, HCO_3^-, Cl^-, and SO_4^{2-} had mean values of 566.1 mg/L, 32.4 mg/L, 200.7 mg/L, 94.1 mg/L, 393.6 mg/L, 665.1 mg/L, and 751.1 mg/L, respectively (Table 1). The mean values of cations and anions showed trends of $Na^+ > Ca^{2+} > Mg^{2+} > K^+$, and $Cl^- > SO_4^{2-} > HCO_3^- > NO_3^-$, respectively. Sodium is the main dominant cation which varied from 110 to 2094.8 mg/L. Calcium is the second most principal cation which varied from 46.4 to 602.4 mg/L with a mean value of 200.7 mg/L. The mean concentrations of magnesium and potassium were 94.1 and 32.4 mg/L, respectively. The concentration of nitrate varied from 3.5 to

178.8 mg/L with a mean of 55.6 mg/L. Spatial distribution map of nitrate contents indicated that NO_3^- content in 50% of groundwater samples exceeds the maximum acceptable value (45 mg/L) for drinking (Fig. 6). Chloride is the main dominant anion with a concentration ranging from 85 to 1992 mg/L, with a mean value of 665.1 mg/L. Sulfate is the second most available anion with a concentration ranging from 51.6 to 3370.2 mg/L and a mean value of 751.1 mg/L. The bicarbonate concentration varied from 72 to 787 mg/L with a mean value of 393.6 mg/L.

For identifying the groundwater types for the studied aquifer, Piper's trilinear diagram (1944) was applied (Fig. 7). According to the chemical composition of the analyzed groundwater samples, three groundwater types were presented by Na–Ca–HCO_3, mixed Ca–Mg–Cl and Na–Cl.

Chadah's classification is also applied to the collected groundwater samples to identify the hydrochemical processes and groundwater facies (Fig. 8). The groundwater samples can

Fig. 5 Spatial distribution map of salinity contents in El Fayoum Depression
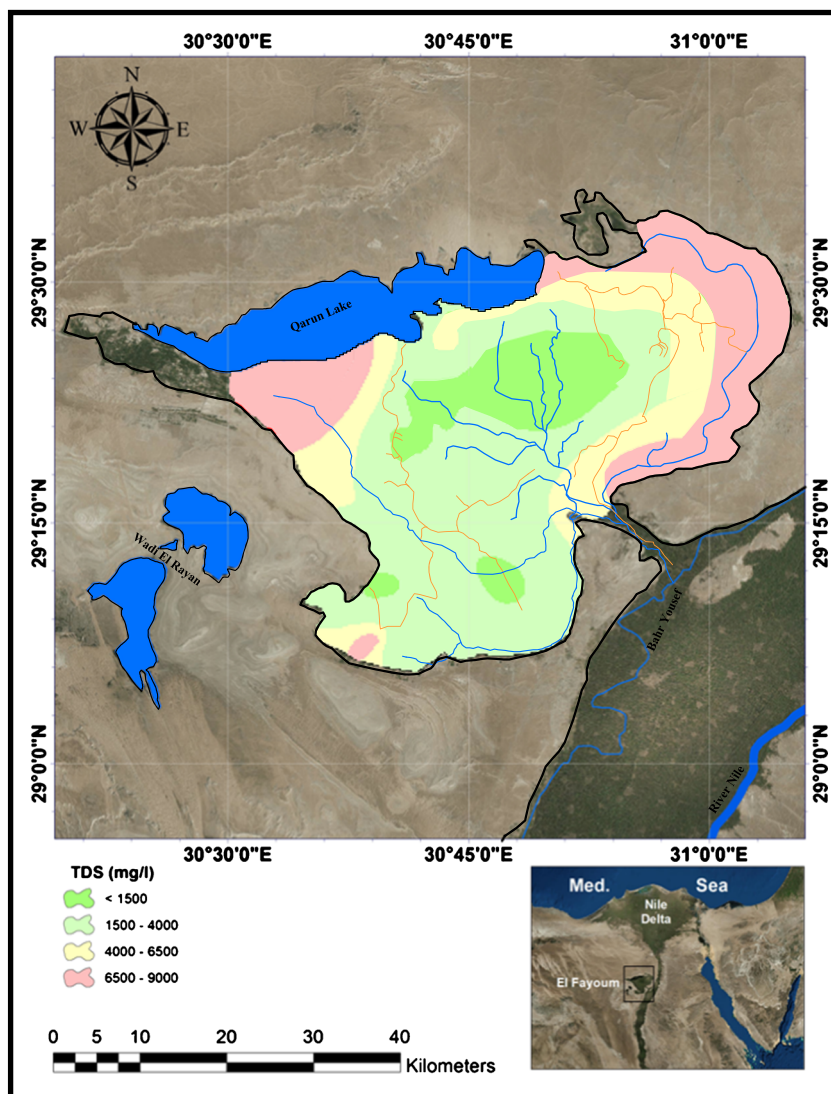
Fig. 6 Spatial distribution map of nitrate (NO_3^-) in El Fayoum Depression
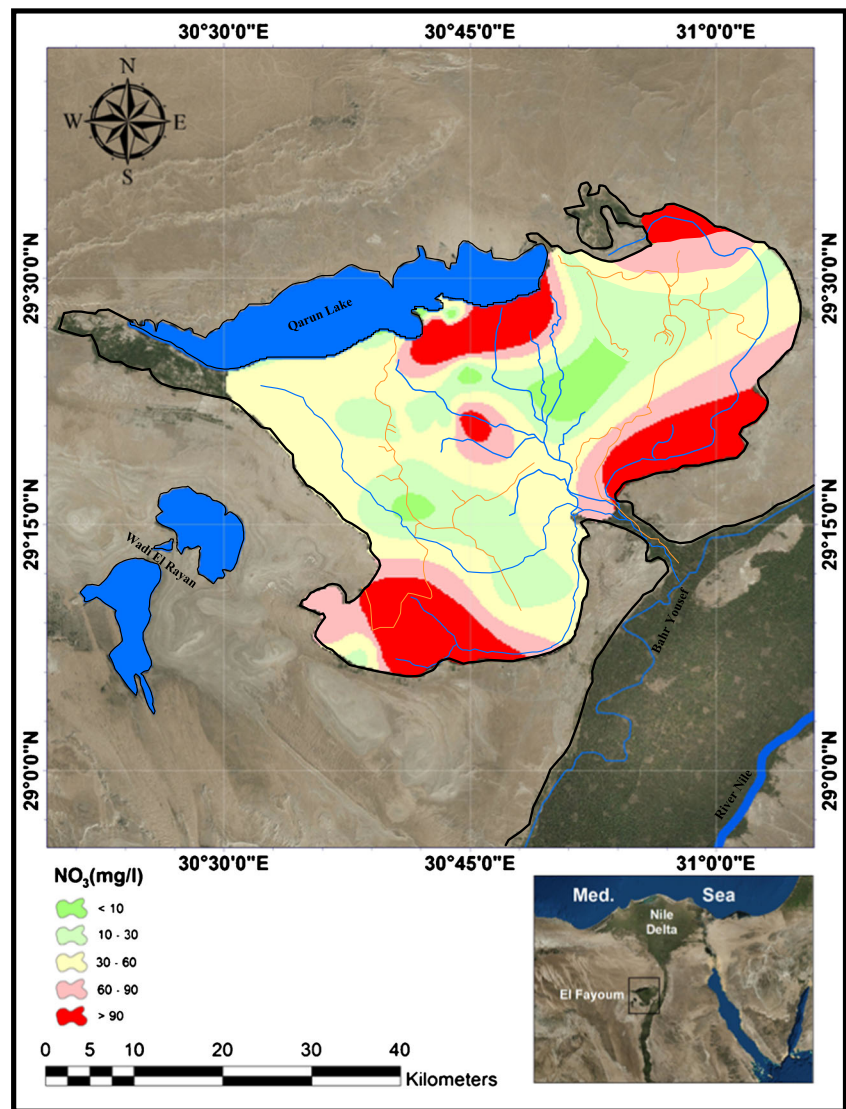
be related to fields 2, 3, and 4. Field 2 indicates reverse ion exchange process, field 3 reveals mixing with saline water, and field 4 shows base ion exchange process.

Statistical analysis

The Correlation matrix (CM) was determined for the physico-chemical parameters of the groundwater samples using Pearson's correlation coefficient to measure the relationships between the analyzed groundwater physicochemical parameters. Correlation coefficient results (Fig. 9) revealed that TDS was strongly correlated with Na^+, Cl^-, SO_4^2, Ca^{+2-}, Mg^{2+}, NO_3^-, HCO_3^-, and K^+ with correlation coefficients (r) of 0.96, 0.96, 0.95, 0.88, 0.87, 0.62, 0.56, and 0.55, respectively, which indicated a similar type of sources (Yang et al. 2016).

The correlations between the major analyzed physicochemical components of the collected groundwater samples

such as TDS, Na^+, K^+, Ca^{2+}, Mg^{2+}, Cl^-, SO_4^{2-}, HCO_3^-, and NO_3^- were identified through the geochemical processes and their controlling mechanisms that influenced the groundwater quality evolution (Fig. 10). Generally, the relation between Na^+ vs. Cl^- is important for the mechanisms identification for acquiring salinity in semi-arid regions like the study area (Fig. 10a). The groundwater samples fell below halite dissolution line with a positive high correlation coefficient ($R^2 = 0.86$) which they reflect ion exchange process or weathering of the silicate minerals. The concentrations of SO_4^{2-} ions increased linearly vs. Cl^- ions concentrations (Fig. 10b), and the groundwater samples were distributed around the mixing line. The (Ca^{2+} + Mg^{2+})–(HCO_3^- + SO_4^{2-}) vs. Na^+–Cl^- plot revealed that the groundwater samples fell on a best fit line with a high correlation coefficient ($R^2 = 0.94$) (Fig. 10c). The relationship between Na^{2+} vs. (Ca^{2+} + Mg^{2+}) revealed that the

Fig. 7 Piper trilinear diagram
showing groundwater types in the
study area
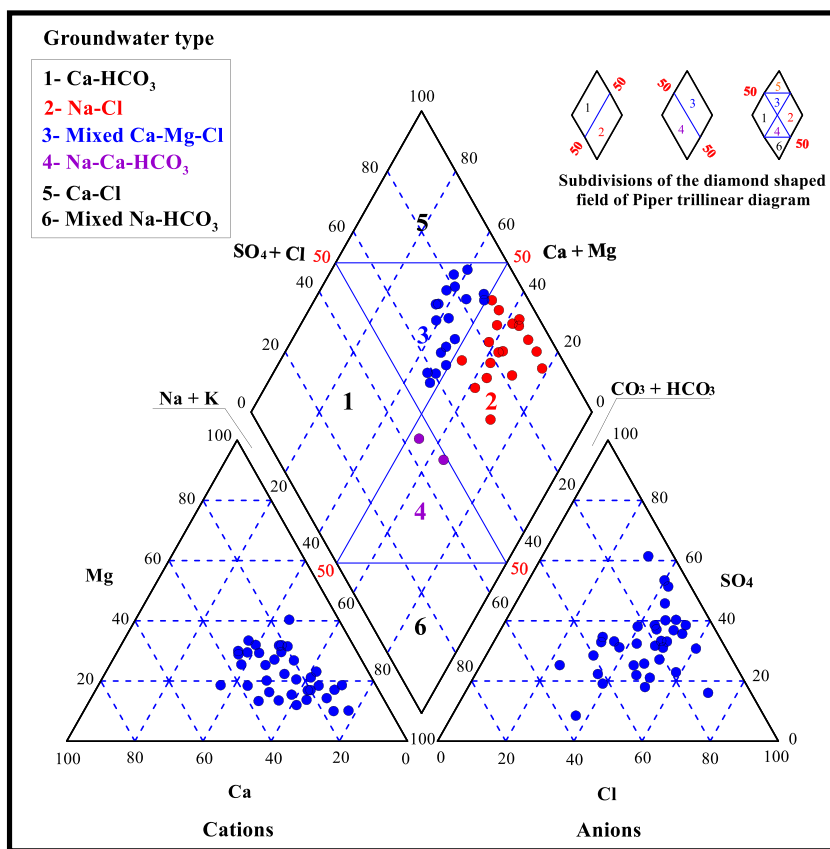
groundwater samples fell around equimolar line (Fig. 10d).
The relation of (SO_4^{2-} + HCO_3^-) vs. (Ca^{2+} + Mg^{2+}) indicated that most of groundwater samples fall below equimolar line (Fig. 10e). The plot of Na^+ vs. SO_4^{2-} (Fig. 10e)
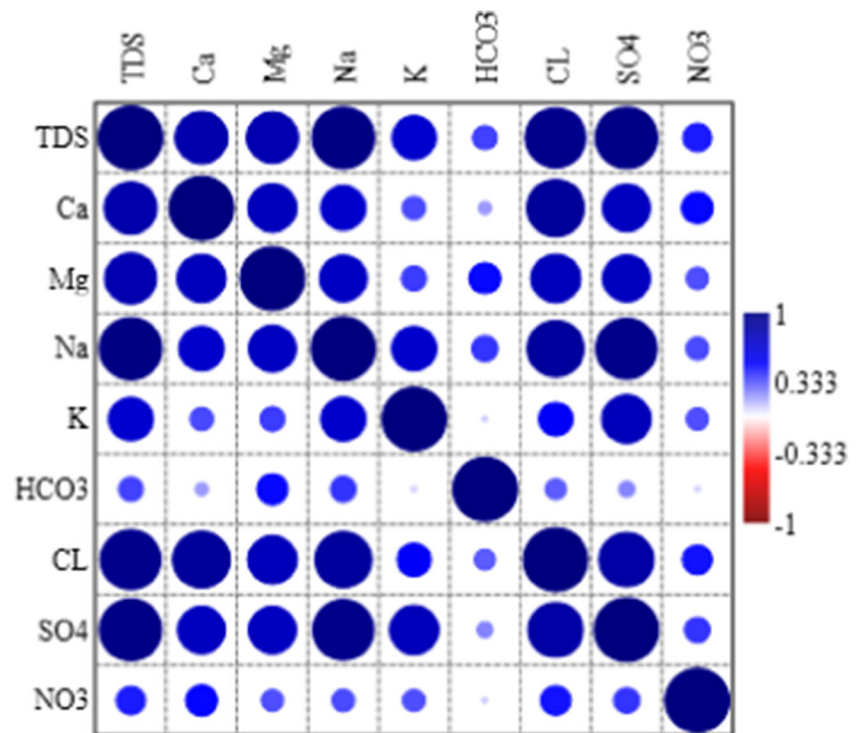showed a high positive correlation coefficient (R^2 = 0.76).

Groundwater mineralization processes

Cation exchange is one of interactions between water and
aquifer materials which greatly affect groundwater's major
ion compositions. Chloro-alkaline indices showed that most

Fig. 8 Geochemical controlling
mechanisms and water facies
(Chadha 1999)
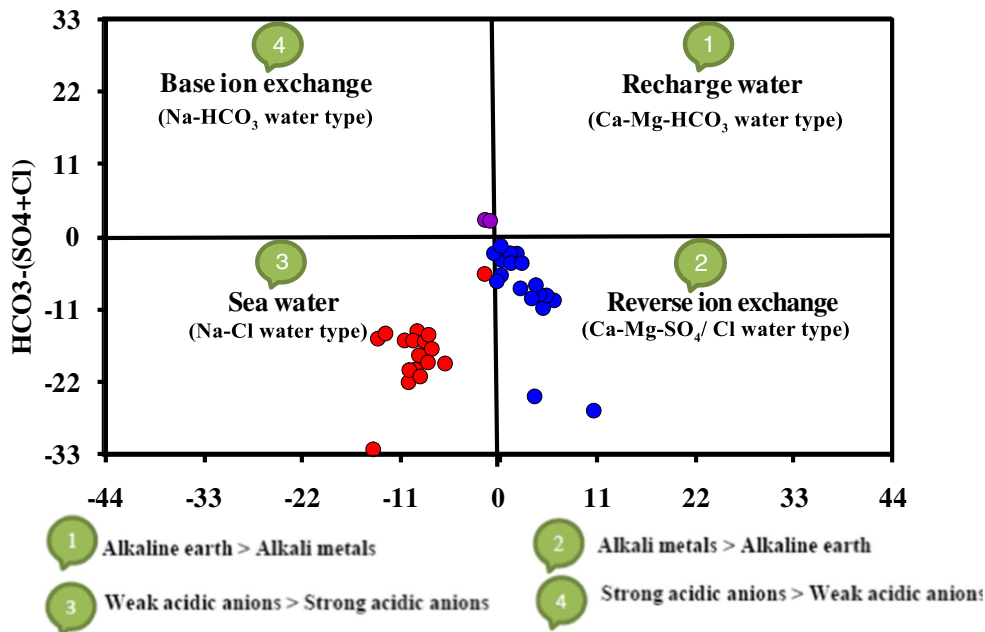
of groundwater samples (68%) were negative sign, while the rest of samples (32%) had positive sign.

The evolution of hydrochemical facies (HFE) diagram (Giménez-Forcada and San Román 2015) reveals processes influences such as dissolution of evaporite sediments from the salt marches, which they are rich in sulfate and chloride in the aquifer matrix (Fig. 11). Twelve groundwater samples located in the area of mixed water showed higher concentrations of calcium and sodium.

The main controlling processes that drive the groundwater chemical composition are recognized using Gibb's diagram by plotting TDS vs. the ratios $Na/(Na + Ca)$ and $Cl/(Cl + HCO_3)$. According to the plot of geochemical data on Gibbs diagram, the groundwater points were scattered in the rock and evaporation dominance fields (Fig. 12).

The dendrogram of the sampling sites (Fig. 13) shows that there are two distinct groups. The first group consists of the groundwater sampling sites (1–38) that have EC ranges from 959.84 to 13984.38 μs/cm, while the second group consists of drainage water sites, which have EC ranges from 1017 to 3546 μs/cm.

The SI was estimated using a geochemical model to improve understanding geochemical processes influencing the overall groundwater quality of the Quaternary aquifer. The obtained results presented SI of 9 minerals and partial pressure of CO_2 for each groundwater sample. Statistical descriptions of the SI results were presented in Table 2. The SI of mineral are in the following order: kaolinite > Ca-montmorillonite > dolomite > gibbsite > calcite > quartz > aragonite > gypsum >

anhydrite > partial pressure of CO_2, with the mean SI of 3.68, 2.85, 1.45, 0.83, 0.69, 0.68, 0.59, − 1.01, − 1.21, and − 2.02, respectively. The geochemical model results revealed that the groundwater in the study area had a high tendency to precipitate the minerals of kaolinite $(Al_2Si_2O_5(OH)_4)$, Ca-montmorillonite $(Ca)_{0.33}(Al, Mg)_2(Si_4O_{10})(OH)_2 \cdot nH_2O)$, dolomite $(Ca, Mg(CO_3)_2$, gibbsite $(Al(OH)_3$, calcite $(CaCO_3)$, quartz(SiO_2), and aragonite $(CaCO_3)$; in addition, the groundwater had the tendency to dissolve minerals of gypsum $(CaSO_4 \cdot 2H_2O)$ and anhydrite $(CaSO_4)$ from aquifer materials (Table 2; Figs. 14 and 15). The obtained values of SI indicated that the groundwater in the study area is supersaturated with calcite, aragonite, dolomite, and quartz, while it is unsaturated with gypsum and anhydrite; in addition, the partial pressure of CO_2 has been negative in value (− 2.023) and below saturation states. The deduced minerals are classified according to the anion part into sulfates, silicates, carbonates, hydroxide, and evaporite minerals.

Groundwater quality indices

The classification of the groundwater samples according to DWQI was presented in Table 4. The obtained results of DWQI showed that all the groundwater samples are not recommended for drinking uses, where about 58% of the groundwater samples have very poor quality for drinking, while the remaining samples (42%) are classified as unsuitable for drinking (Table 4). The spatial distribution of the obtained quality classes based on DWQI was presented in Fig. 16.
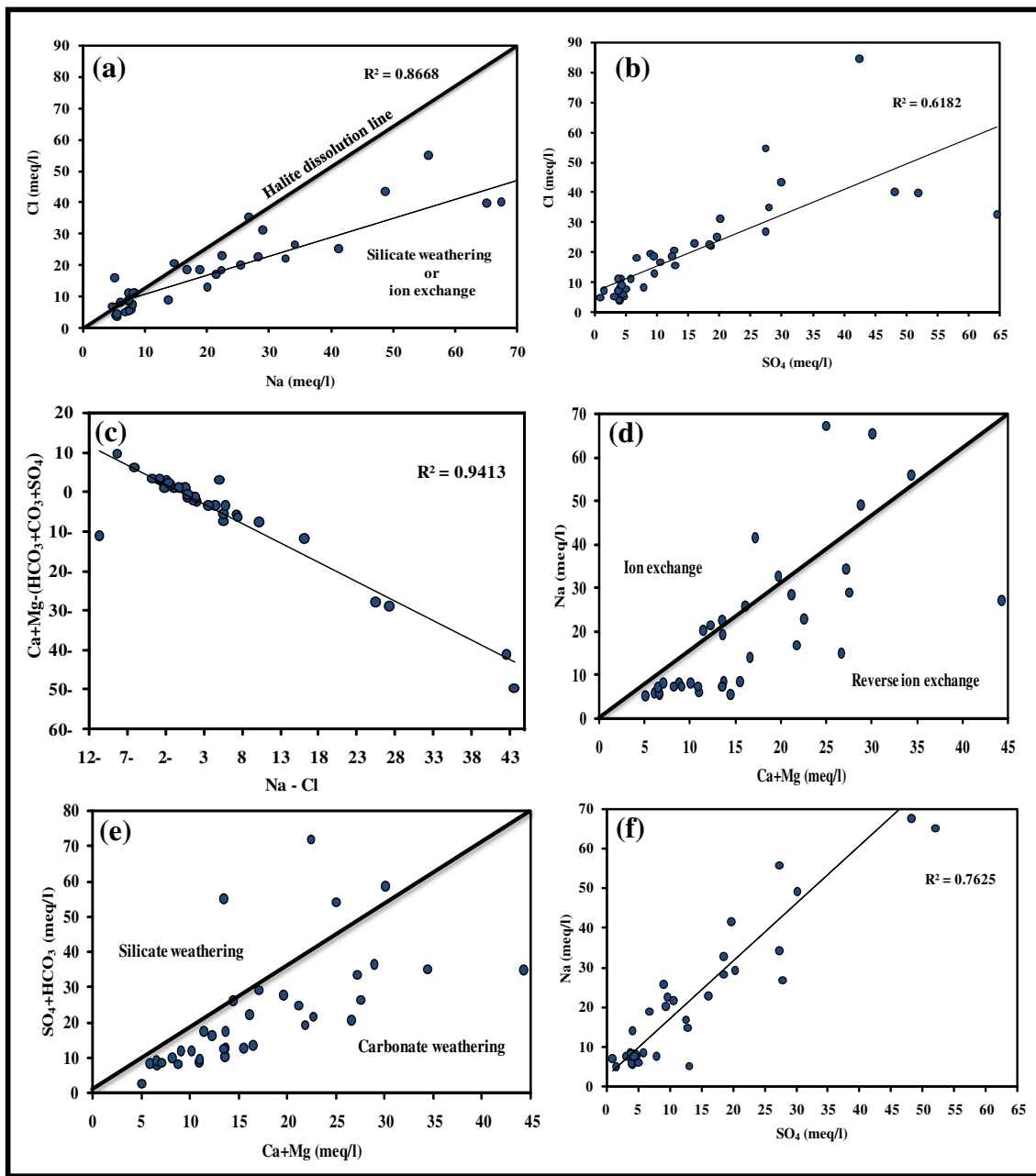
Fig. 10 Relationships between major ions and their ionic ratios for the collected groundwater samples

For irrigation use, the groundwater samples were classified using five hazard groups depending on the rates and weights of the physicochemical parameters (Tables 5, 6, and 7). The IWQI was calculated by a linear combination of these hazard groups, as presented statistically in Table 8. The IWQI values of the collected groundwater samples range from 26.1 to 36.1, indicating a medium class of quality for irrigation purposes (Table 9). The spatial distribution map of IWQI showed that the groundwater quality for irrigation decreased toward the northeastern and southern parts of the depression (Fig. 17). In addition, the SAR ranges from 1.89 to 48.71, with a mean value of 8.03. According to SAR classification, the SAR values revealed that about 79% of the groundwater samples fall in excellent class for irrigation usage (SAR: 2–10), and approximately 13% of samples fall in good class for irrigation (SAR: 10–18), while about 5% of samples fall in doubtful or fairly poor water for irrigation (SAR: 18–26) and the rest of samples about 3% fall in unsuitable class for irrigation usage (SAR: > 26).

**Fig. 11** Hydrochemical facies evolution diagram (HFE) for the collected samples
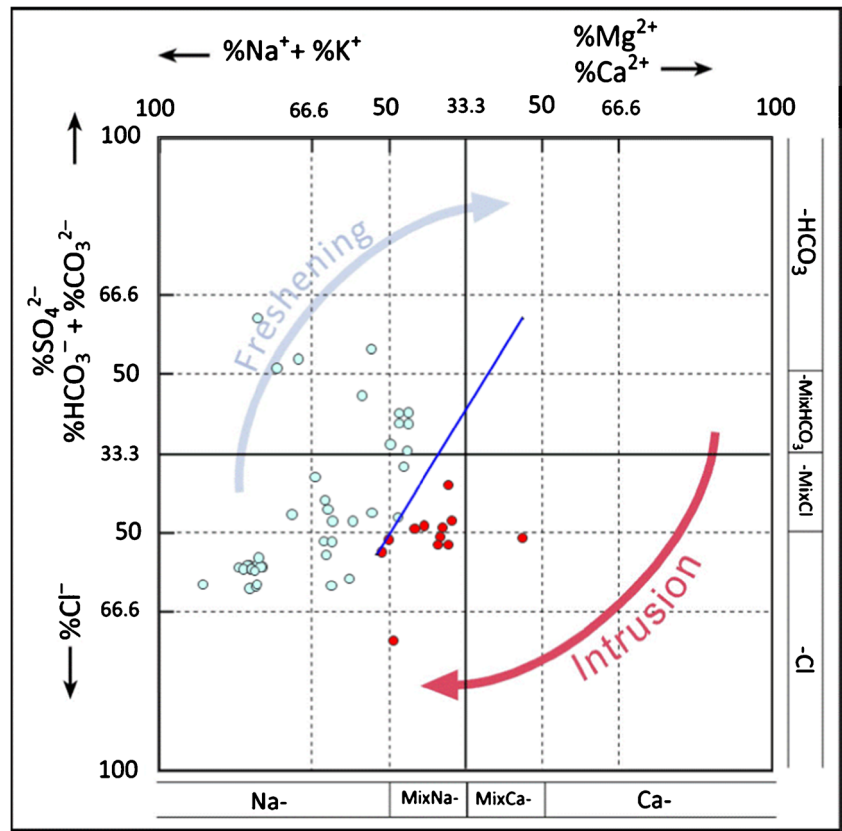

Discussion

Chemical analysis of the groundwater resources can be used to define and monitor geochemical processes influencing the composition of groundwater in the study area, such as dissolution, precipitation, and ion exchange reactions that reflects variation in water quality. For example, the relatively high values of TDS may be related to rock–water interaction, the recharge from the underlying fractured limestone of the Eocene aquifer, the irrigation return flow, and seepage from drains (El Sheikh 2004). As indicated by the spatial distribution map of salinity (Fig. 5), the TDS increases radially from the central part of the study area towards the peripheries that dissected by many drains, where the seepage from drains leads to increase the groundwater salinity, unlike the central part that is dissected by many canals. In addition, the decreasing of the Quaternary aquifer thickness radially from the central part towards the peripheries, where its minimum thickness is found, may also increase the groundwater salinity (Ahmed 2012).

Fig. 12 Gibbs diagram for the collected groundwater samples in El Fayoum Depression
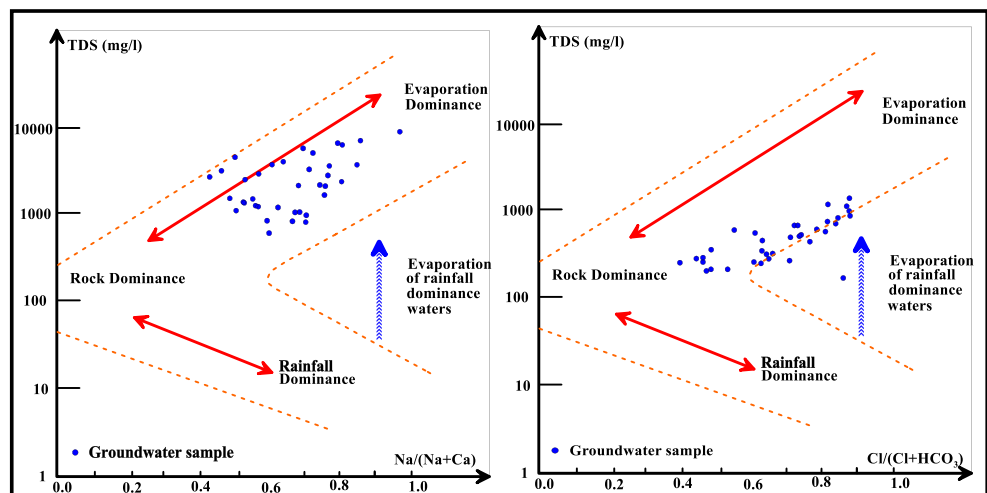
Fig. 13 Hierarchical cluster analysis (HCA) of the sampled waters
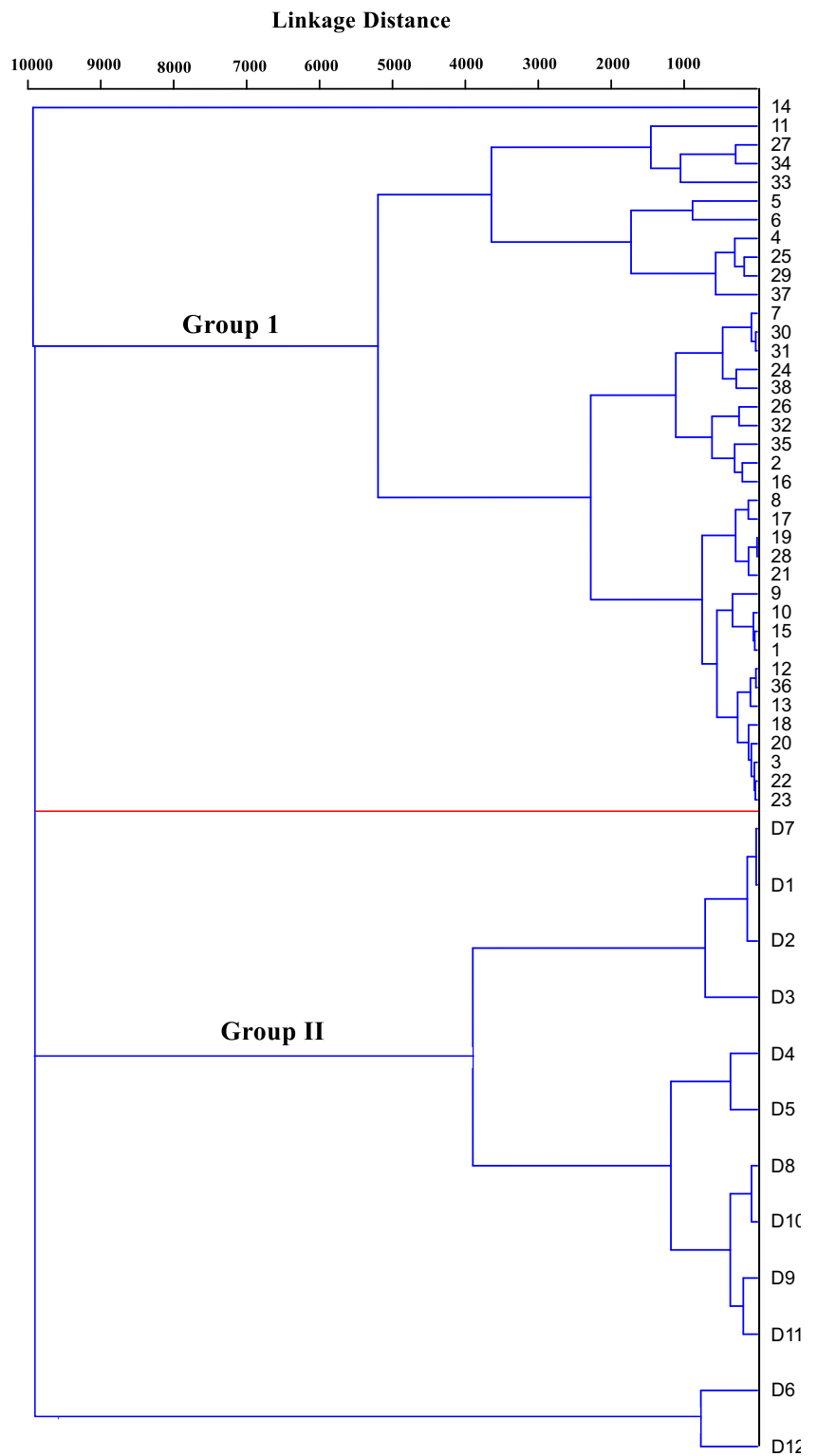
The majority of the population in the study regions relies on agricultural practices for living, using various fertilizers for crop yields, suggesting that the influence of anthropogenic activities, consisting of irrigation, which tends to apply more

of nitrate-based fertilizers, and domestic wastes in the study area (Adimalla et al. 2018). Debernardi et al. (2008) analyzed nitrate concentrations in groundwater and considered the substantial use of fertilizers as the main explanation for the
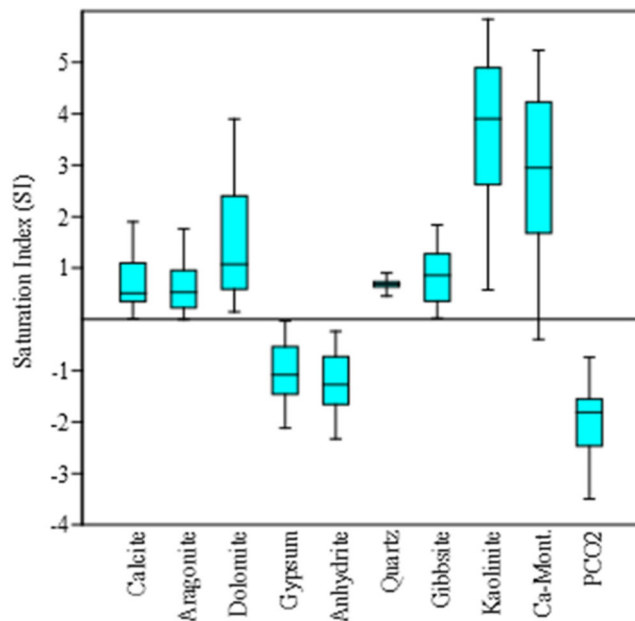
Fig. 14 Box plot of the relevant minerals saturation index

elevated NO_3^- concentrations. Figure 6 indicated that the pollution by nitrate exceeded the acceptable limit for drinking (45 mg/L) around the periphery of and near Qarun Lake that may cause a high health risk to humans and harmful diseases.

Geochemical facies and controlling mechanisms

The major ion concentrations are powerful tools to detect the solute sources, where the wide ranges of the determined ions in the groundwater samples indicated the influence of various recharging sources, e.g., surface canals, drains and irrigation return flow, anthropogenic activities, and excessive use of fertilizers and pesticides (Jalali 2007).

The prevailing water types in the study area as shown by Piper diagram (Fig. 7) are Na–Cl, mixed Ca-Mg-Cl, and Na-Ca-HCO$_3$ facies; in addition, the tendency of the groundwater to precipice calcite, aragonite (CaCO$_3$), and dolomite (CaMg(CO$_3$)$_2$ and dissolve gypsum (CaSO$_4$·2H$_2$O) and anhydrite (CaSO$_4$) (Table 2) indicated that the groundwater was affected by leaching, mineral dissolution, ion exchange, and evaporation processes (Bhat et al. 2016).

The results obtained from Piper diagram are in good agreement with the results of Chadha diagram (Fig. 8) and confirmed that the groundwater quality in the study is mainly controlled by the dissolved Na$^+$ and K$^+$ and reverse ion exchange processes between Ca^{2+} and Mg^{2+} in clay aquifer matrix due to irrigation return flow, seepage from drains, and water–rock interaction, where the study area is mostly covered by the Quaternary sediments that have a fluvio-lacustrine origin, and are composed of sand and gravel with silt and clay intercalations. The strong correlation between Na$^+$, Cl$^-$, SO$_4^{2-}$, Ca^{+2-}, Mg^{2+}, NO$_3^-$, HCO$_3^-$, and K$^+$ (Table 3) indicated similar sources for these ions (Yang et al. 2016).

The relation between Na$^+$ vs. Cl$^-$ (Fig. 10a) indicated that the groundwater samples fell below halite dissolution line reflecting the effect of the ion exchange process or weathering of the silicate minerals on the groundwater chemistry. The linear increasing of SO$_4^{2-}$ ions with Cl$^-$ ion concentrations (Fig. 10b) reflects effect of the dissolution process of gypsum and anhydrite minerals. The plot of (Ca^{2+} + Mg^{2+})–(HCO$_3^{2-}$ + SO$_4^{2-}$) vs. Na$^+$–Cl$^-$ (Fig. 10c) revealed that the ion exchange is a principal geochemical reaction in controlling the groundwater chemistry. The relation between Na^{2+} vs. (Ca^{2+} + Mg^{2+}) (Fig. 10d) reflects the ion exchange process and oversaturation of calcite, aragonite, and dolomite minerals. The relation of (SO$_4^{2-}$ + HCO$_3^-$) vs. (Ca^{2+} + Mg^{2+}) reflects the carbonate and silicate weathering (Fig. 10e). The plot of Na$^+$ vs. SO$_4^{2-}$ (Fig. 10e) reflects the intercalation between groundwater and aquifer materials. The irrigation return flow and the human activities could be the major source of high concentration of nitrate contents in the shallow groundwater

Fig. 15 Scattered plot of minerals saturation indices vs.TDS
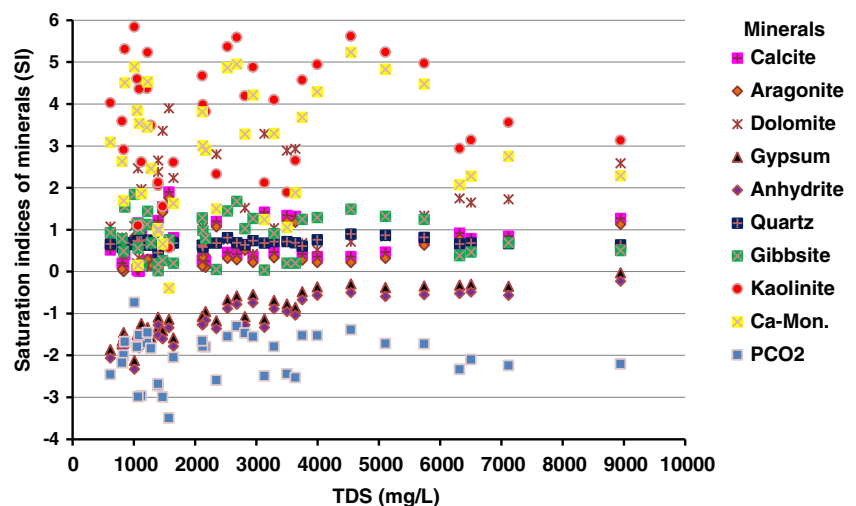
Table 4 Drinking water quality index (DWQI) classification according to arithmetic rating method

DWQI	Class	Well no.
0–25	Excellent water	
26–50	Good water	
51–75	Poor water	
76–100	Very poor water	1, 2, 4, 6, 7, 8, 9, 10, 11, 12, 13, 14, 15, 16, 17, 18, 19, 20, 21, 22, 23, 24
> 100	Unsuitable water	3, 5, 25, 26, 27, 28, 29, 30, 31, 32, 33, 34, 35, 36, 37, 38

resources, as a result of the oxidation of nitrogenous compounds within the aquifer materials and fixation through microorganisms and leguminous plants (Jalali 2005; Chica-Olmo et al. 2017).

The reverse ion exchange has a main role in controlling the groundwater chemistry as indicated by results of the Chloroalkaline indices. The majority of the groundwater samples have negative CAI value, where the alkaline earth ions (Ca and Mg ions) dissolved in groundwater have been exchanged with alkaline metal ions (Na and K) in aquifer matrix as a process according to Eq. (15). However, the presence of clay and shale in aquifer matrix in contact with groundwater have adsorb Na and K ions, and thus, alkaline earth metals (Ca and Mg ions) are released into the groundwater indicating ion exchanges process affecting the groundwater samples with positive CAI values according to Eq. (16).

Fig. 16 Spatial distribution map of DWQI according to arithmetic rating method
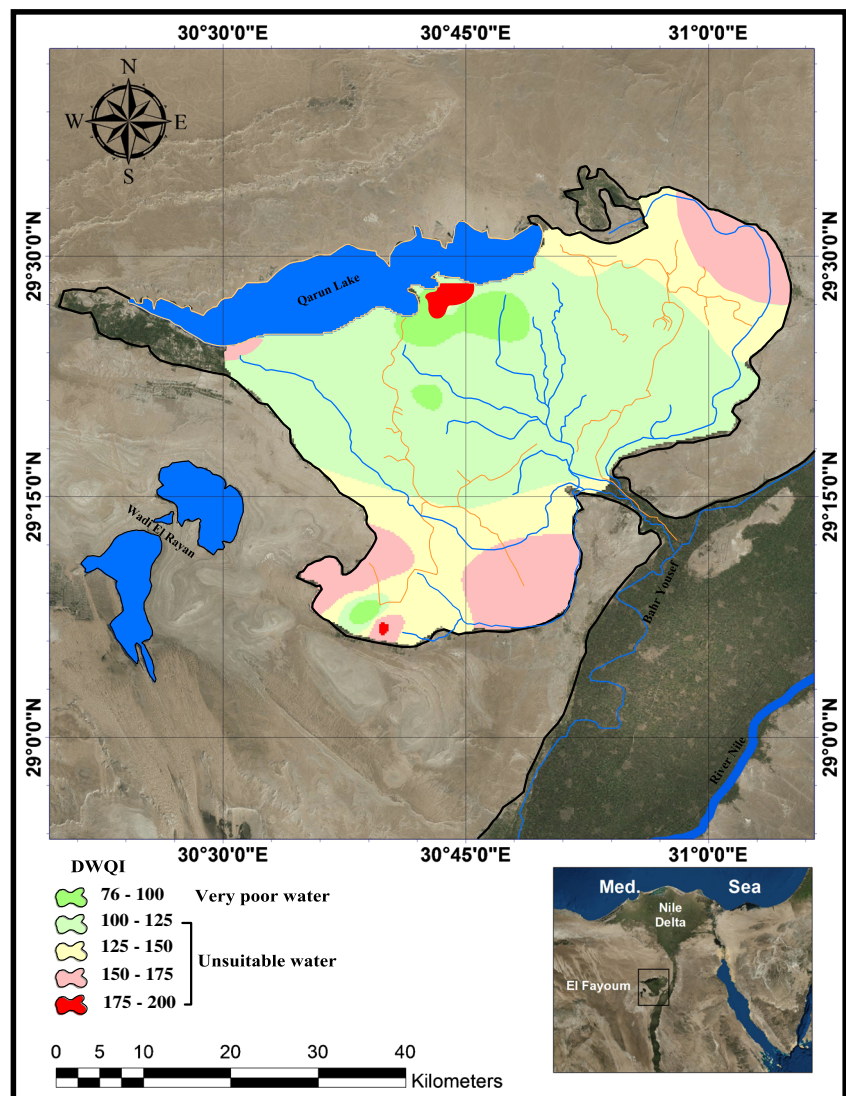
Table 5 Groundwater suitability for irrigation according to the hazard groups classification based on rate and weight

Hazard	Weight	Parameter	Range	Rating	Suitability	Samples (%)
Salinity hazard	5	Electrical conductivity (μS/cm)	EC < 700	3	High	Nil
			700 ≤ EC ≤ 3000	2	medium	50%
			EC > 3000	1	Low	50%
Infiltration and permeability hazard	4	Electrical conductivity (μS/cm) with Sodium adsorption ratio	See Table 6 for details	3	High	100%
				2	medium	Nil
				1	Low	Nil
Specific ion toxicity	3	Sodium absorption ratio (−)	SAR < 3.0	3	High	18%
			3.0 ≤ SAR ≤ 9.0	2	medium	58%
			SAR > 9.0	1	Low	24%
		Chloride (mg/l)	CI < 140	3	High	18%
			140 ≤ CI ≤ 350	2	medium	18%
			CI > 350	1	Low	63%
Trace element toxicity	2	Al, Cu, Cr, Cd, Mn, Fe, Ni and Pb (mg/l)	See Table 7 for details	3	High	100%
				2	medium	Nil
				1	Low	Nil
		Se (mg/l)		3	High	21%
				2	medium	79%
				1	Low	Nil
Miscellaneous effects to sensitive crops	1	Nitrate Nitrogen (mg/l)	NO_3–N < 5.0	3	High	32%
			$5.0 ≤ NO_3$–N ≤ 30.0	2	medium	58%
			NO_3–N > 30.0	1	Low	11
		Bicarbonate (mg/l)	HCO_3 < 90	3	High	5%
			$90 ≤ HCO_3 ≤ 500$	2	medium	82%
			HCO_3 > 500	1	Low	13%
		pH	7.0 ≤ pH ≤ 8.0	3	High	Nil
			6.5 ≤ pH < 7.0 and 8.0 < pH ≤ 8.5	2	medium	5%
			pH < 6.5 or pH > 8.5	1	Low	95%

$$Na^+(Groundwater) + \frac{1}{2} \ Ca^{2+}(Aquifer \ matrix) \rightarrow Na^+(Aquifer \ matrix) + \frac{1}{2} \ Ca^{2+}(Groundwater) \qquad (15)$$

$$\frac{1}{2} \ Ca^{2+}(Groundwater) + Na^+(Aquifer \ matrix) \rightarrow \frac{1}{2} \ Ca^{2+}(Aquifer \ matrix) + Na^+(Groundwater) \qquad (16)$$
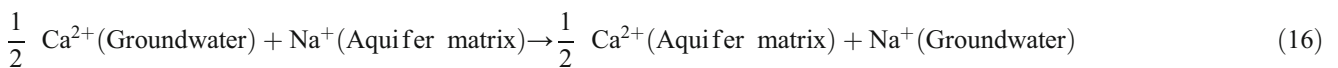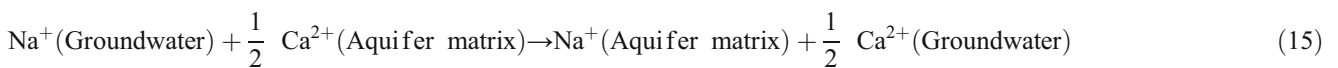
Table 6 Infiltration and permeability hazard group classification according to rate

		Sodium absorption ratio (SAR)					Rate	Suitability
	EC	< 3	3–6	6–12	12–20	> 20		
		> 700	> 1200	> 1900	> 2900	> 5000	3	High
		700–200	1200–300	1900–500	2900–1300	5000 –2900	2	Medium
		< 200	< 300	< 500	< 1300	< 2900	1	Low

Table 7 Classification of trace element toxicity (Simsek and Gunduz 2007)

Trace element (mg/l)	Range	Rating	Suitability
Al	Al > 5.0	3	High
	5.0 ≤ Al ≤ 20	2	Medium
	Al > 20.0	1	Low
Cu	Cu > 0.2	3	High
	0.2 ≤ Cu ≤ 5.0	2	Medium
	Cu > 5.0	1	Low
Cr	Cr > 0.1	3	High
	0.1 ≤ Cr ≤ 1.0	2	Medium
	Cr > 1.0	1	Low
Cd	Cd > 0.01	3	High
	0.01 ≤ Cd ≤ 0.05	2	Medium
	Cd > 0.05	1	Low
Mn	Mn > 0.2	3	High
	0.2 ≤ Mn ≤ 10.0	2	Medium
	Mn > 10.0	1	Low
Fe	Fe > 5.0	3	High
	5.0 ≤ Fe ≤ 20	2	Medium
	Fe > 20.0	1	Low
Ni	Ni > 2.0	3	High
	0.2 ≤ Ni ≤ 2.0	2	Medium
	Ni > 2.0	1	Low
Pb	Pb > 0.5	3	High
	0.5 ≤ Pb ≤ 10	2	Medium
	Pb > 10.0	1	Low
Se	Se > 0.01	3	High
	0.01 ≤ Se ≤ 0.02	2	Medium
	Se > 0.02	1	Low

Table 9 Irrigation water quality index classification (Simsek and Gunduz 2007)

IWQI	Suitability for irrigation	Samples (%)
< 22	Low	Nil
22–37	Medium	100%
> 37	High	Nil

magnesium and calcium in the groundwater (Kawoa and Karuppannanb 2018). Therefore, cation exchange processes effects on evolution of groundwater quality in the study area, which confirmed with the prevailing water types in the study area such as, Na-Ca-HCO$_3$, mixed Ca–Mg–Cl and Na–Cl facies as reported by Piper diagram. So, the two processes can be the variables that govern the area's chemical groundwater composition.
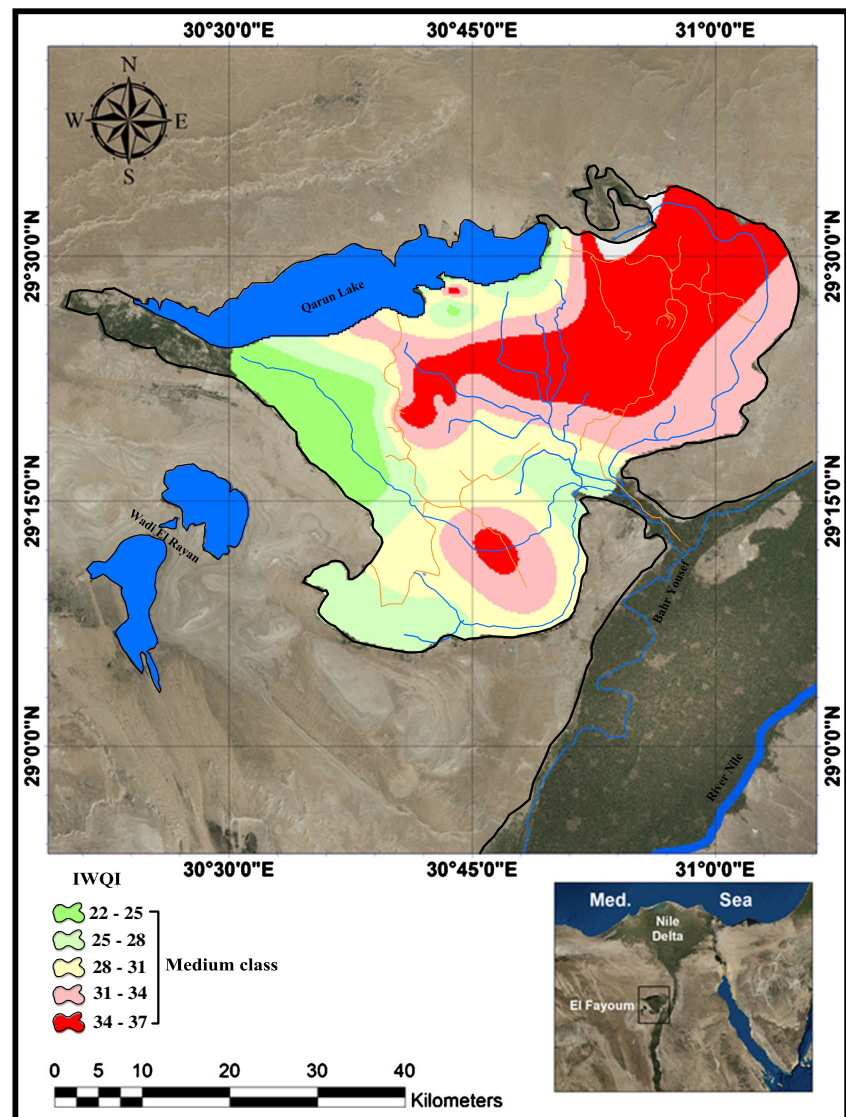
The obtained result of HFE diagram (Fig. 11) indicates the effect of two significant geochemical processes controlling groundwater geochemistry since high concentrations of bicarbonate and calcium ions indicated rock–water interaction processes, while high concentrations of chloride and sodium ions indicated evaporation processes (Giménez-Forcada and San Román 2015; Bouderbala and Gharbi Ben 2017; Kanagaraj et al. 2018).

Gibbs diagram (Fig. 12) indicated that most groundwater samples fall in rock dominant zone, and the chemistry of groundwater is influenced by rock dominance and rock water interaction. This indicates groundwater chemistry is influenced by rock dominance and the long time contact between rock and water.

In addition, the groundwater samples display a slight tendency towards the prevailing evaporation region, which suggests increased concentration of TDS and chloride in the groundwater as a result of the incremental effects of liquid wastes, seepage from drains, and irrigation return flow. Therefore, the groundwater samples can move towards the evaporation field from the rocky field. These mechanisms indicate that the quality of the original groundwater of geographic origin has become semi-salty water (brackish) due to the influence of human activities on the aquifer system.

According to the CA results, the cluster classifications varied with significance levels between groups I and II, which presented in Fig. 13. This is also confirmed by the significant differences in the mean values of EC among groundwater and drainage waters. The location of groundwater sites indicates that these sites have chemical characteristics similar to drainage waters. At some localities in Fayoum Depression, the mixing of drainage waters with groundwater causes dilution of the dissolved salts and consequently similar physicochemical chemical characteristics of the samples. According to groups I and II, the groundwater sample differs from the others in salinity, which might be due to the position of this

This review of CAI indicates that the cation/ion exchange is the key mechanism that influences the groundwater chemistry in the study area. It reveals that the cation exchange, such as potassium and sodium in groundwater, is replaced with magnesium and calcium from the water bearing formation during the contact time of water with the aquifer material (Xiao et al. 2012); hence, the reverse ion exchange happens between potassium and sodium in the formation with

Table 8 Statistical description of irrigation water quality index (IWQI)

Group	G1	G2	G3	G4	G5	IWQI
Min	5.00	8.00	2.00	5.57	1.33	26.190
Max	15.00	12.00	6.00	6.00	2.33	36.190
Mean	7.63	11.89	3.50	5.87	1.72	30.634
Stand. Dev	2.78	0.64	1.17	0.07	0.25	3.656

Fig. 17 Spatial distribution map of IWQI according to arithmetic rating method

site close to the irrigation drainage waters, in addition percolation from the underlying fractured limestone of the Eocene aquifer exists (El Sheikh 2004).

Geochemical modeling and mineralization processes

Rock-water interaction that affects the aquifers systems is inferred by the obtained results of the geochemical model (NETPATH). The SI of minerals indicated the presence of different hydrogeological environments (Figs. 14 and 15; Table 2). The positive SI values of carbonate minerals (dolomite, calcite, and aragonite) indicate that the groundwater was capable of precipitate from the groundwater, which account for the depletion of dissolved Al and SO$_4$. Therefore, precipitations of such minerals are possible, which account for the depletion of the dissolved Ca and Mg ions. The negative values of SI of sulfate minerals

(gypsum and anhydrite) indicate the ability of groundwater in the study area to dissolve those minerals and, consequently, they accept more Ca and SO$_4$ constituents. The same water is oversaturated with gibbsite mineral phases, which accounts for the decrease of the dissolved Al and SO$_4$ through the precipitation process.

The saturation indices of the relevant minerals reflected the effect of geochemical processes such as leaching, dissolution, precipitation, ion exchange in controlling of the evolution groundwater chemistry, and the hydrochemical properties of the aquifer system (El Kadi et al. 2011). The negative value of PCO$_2$ reflects the recharge from the underlying aquifer, the irrigation return flow, and seepage from drains.

According to Fig. 14 and 15, precipitation is clearly proved as the carbonates were exaggeratedly saturated in all groundwater samples. Although the saturation process was obtained in limited samples regarding anhydrite and gypsum, revealing

equilibrium, the evaporation process dominates the unsaturation state, especially halite, which reflects the dissolution of evaporation in most groundwater samples. With respect to this process, gypsum and anhydrite are continuously dissolved without precipitation, which results in increased Ca^{2+} concentration and a decrease in the concentrations of HCO_3^- and CO_3^{2-} by precipitation of calcium carbonate. Thus, evaporation plays no important role in groundwater chemistry, while the dissolution of carbonates often affects water chemistry.

Groundwater quality assessment

The obtained results of DWQI showed that the groundwater in the study area cannot be recommended for drinking uses, since the groundwater samples come under the very poor to unsuitable water quality category for drinking (Table 4). Accordingly, the groundwater in the study area should be treated before it can be used for drinking purposes. For irrigation usages, the groundwater samples have a medium quality according to IWQI classification (Table 5). As indicated by SAR results, the high concentrations of Na^+ in groundwater samples, compared with Ca^{2+} and Mg^{2+}, are absorbed by the soil, causing the soil permeability decreasing, degradation of soil structure, and stunting plant growth (Richards 1954). Therefore, a special treatment is required before use according to the types of crops.

The groundwater quality is a result of chemical composition of recharge sources, mineral composition of aquifer formation, rock-water interaction, and the anthropogenic activities that lead to water quality deterioration for drinking and irrigation usages (Li et al. 2017). The deterioration of the groundwater quality for drinking and irrigation in the study area may be attributing to the poor drainage network and contamination by irrigation return flow and seepage from drains through some geochemical processes resulting from rock water interaction such as reverse ion exchange, leaching, dissolution and precipitation processes.

Conclusions

For evaluation of the geochemical processes regulating groundwater quality in the Quaternary aquifer of El Fayoum Depression, physicochemical parameters were determined for the collected groundwater samples. According to the obtained results, groundwater in the investigated area belongs to Na–Cl, mixed Ca–Mg–Cl, and Na–Ca–HCO_3 water types. These compositions reflect the effects of leaching, dissolution of evaporite deposits, and anthropogenic activities in areas close to the Nile River. The SI of minerals indicated the presence of different hydrogeological environments. The SI of the relevant minerals reflected the effect of geochemical processes

such as leaching of the aquifer materials and cation exchange processes.

The results of DWQI indicated that all the groundwater samples are not suitable for drinking. The IWQI results showed that all groundwater samples were in the medium quality class for irrigation suitability. The deterioration of the groundwater quality could be attributed to high mineralization processes resulting from aquifer materials; in addition, contamination by irrigation return flow through high application of agrochemical pesticides and the seepage from irrigation drainage canals.

Utilization of physicochemical parameters, geochemical modeling, and WQIs with the help of statistical analysis and GIS techniques is effective and applicable approach and gives a clear picture for the groundwater quality and controlling mechanisms

Compliance with ethical standards

Conflict of interest The authors declare that they have no conflict of interest.

References

Abdel Kawy WA, Belal A (2012) Spatial analysis techniques to survey the heavy metals content of the cultivated land in El-Fayoum Depression, Egypt. Arab J Geosci 5:1247–1258. https://doi.org/10.1007/s12517-011-0312-9

Abd-Elmabod SK, Bakr N, Muñoz-Rojas M, Pereira P, Zhang Z, Cerdà A, Jordán A, Mansour H, De la Rosa D, Jones L (2019) Assessment of soil suitability for improvement of soil factors and agricultural management. Sustainability 11:1588. https://doi.org/10.3390/su11061588

Adimalla N, Li P, Venkatayogi S (2018) Hydrogeochemical evaluation of groundwater quality for drinking and irrigation purposes and integrated interpretation with water quality index studies. Environ Process 5(2):363–383

Ahmed MA (2012) Assessment of intrinsic vulnerability to contamination for the alluvial aquifer in El-Fayoum Depression using the DRASTIC Method. J Radiat Res Appl SC 5(4):743–768

Ammar FH, Chkir N, Zouari K, Hamelin B, Deschamps P, Aigoun A (2014) Hydrogeochemical processes in the complex Terminal aquifer of southern Tunisia: an integrated investigation based on geochemical and multivariate statistical methods. J Afr Earth Sci 100: 81–95. https://doi.org/10.1016/j.jafrearsci.2014.06.015

APHA (2012) Standard methods for the examination of water and wastewater. Amer Public Health Assoc, Washington

Attia AH, El-Sayed SA, El-Sabagh ME (2018) Utilization of GIS modeling in geoenvironmental studies of Qaroun Lake, El Fayoum Depression, Egypt. J Afr Earth Sci 138:58–74. https://doi.org/10.1016/j.jafrearsci.2017.10.010

Ayers R, Westcot D (1994) Water quality for agriculture. FAO Irrigation and Drainage Paper 29 Rev. 1. Food and Agriculture Organization of the United Nations, Rome.

Baioumy HM, Kayanne H, Tada R (2010) Reconstruction of lake level and climate changes in Lake Qarun, Egypt, during the last 7000 years. J Great Lakes Res 36:318–327. https://doi.org/10.1016/j.jglr.2010.03.004

Bartzas G, Tinivella F, Medini L, Zaharaki D, Komnitsas K (2015) Assessment of groundwater contamination risk in an agricultural area in north Italy. Inf Process Agric 2:109–129. https://doi.org/10.1016/j.inpa.2015.06.004

Bhat AN, Bhat AA, Nath S, Singh PB, Guha BD (2016) Assessment of drinking and irrigation water quality of surface water resources of South-West Kashmir, India. J Civil Environ Eng 6(2):222–229. https://doi.org/10.4172/2165-784X.1000222

Bora M, Goswami DC (2017) Water quality assessment in terms of water quality index (DWQI): case study of the Kolong River, Assam, India. Appl Water Sci 7(6):3125–3135. https://doi.org/10.1007/s13201-016-0451-y

Bouderbala A, Gharbi Ben Y (2017) Hydrogeochemical characterization and groundwater quality assessment in the intensive agricultural zone of the Upper Cheliff plain, Algeria. Environ Earth Sci 76:744. https://doi.org/10.1007/s12665-017-7067-x

Bozdag A, Goçmez G (2013) Evaluation of groundwater quality in the Cihanbeyli basin, Konya, Central Anatolia, Turkey. Environ Earth Sci 69(3):921–937. https://doi.org/10.1007/s12665-012-1977-4

Chadha DK (1999) A proposed new diagram for geochemical classification of natural waters and interpretation of chemical data. Hydrogeol J 7:431–439. https://doi.org/10.1007/s100400050216

Chaurasia AK, Pandey HK, Tiwari SK, Prakash R, Pandey P, Ram A (2018) Groundwater Quality assessment using Water Quality Index (DWQI) in parts of Varanasi District, Uttar Pradesh, India. J Geol Soc India 92(1):76–82. https://doi.org/10.1007/s12594-018-0955-1

Chica-Olmo M, Peluso F, Luque-Espinar JA (2017) A methodology for assessing public health risk associated with groundwater nitrate contamination: a case study in an agricultural setting (southern Spain). Environ Geochem Health 39(5):1117–1132. https://doi.org/10.1007/s10653-016-9880-7

Chukwuma CE, Chukwuma CG, Uba IJ, Orakwe CL, Ogbu NK (2016) Irrigation water quality index assessment of Ele River in Parts of Anambra State of Nigeria. Int J Curr Res 4(3):1–6. https://doi.org/10.9734/ACRI/2016/25885

Debernardi L, Luca DAD, Lasagna M (2008) Correlation between nitrate concentration in groundwater and parameters affecting aquifer intrinsic vulnerability. Environ Geol 55:539–558. https://doi.org/10.1007/s00254-007-1006-1

Dhanasekarapandian M, Chandran S, Devi DS, Kumar V (2016) Spatial and temporal variation of groundwater quality and its suitability for irrigation and drinking purpose using GIS and DWQI in an urban fringe. J Afr Earth Sci 124:270–288. https://doi.org/10.1016/j.jafrearsci.2016.08.015

Egbueri JC (2018) Assessment of the quality of groundwater proximal to dumpsites in Awka and Nnewi metro-polises: a comparative approach. Int J Energ Water Res 2(1):33–48. https://doi.org/10.1007/s4210.8-018-0004-1

El Kadi A, Plummer L, Aggarwal P (2011) NETPATH-WIN: an interactive user version of the mass-balance model NETPATH. Ground Water 49(4):593–599. https://doi.org/10.1111/j.1745-6584.2010.00779.x

El Osta M, Masoud M, Ezzeldin H (2020) Assessment of the geochemical evolution of groundwater quality near the El Kharga Oasis, Egypt using NETPATH and water quality indices. Environ Earth Sci 79:56. https://doi.org/10.1007/s12665-019-8793-z

El-Sayed SA, Moussa EMM, El-Sabagh MEI (2015) Evaluation of heavy metal content in Qaroun Lake, El-Fayoum, Egypt. Part I: Bottom sediments. J Radiat Res 8:276–285. https://doi.org/10.1016/j.jrras.2015.02.011

El Sheikh AE (2004) Water budget analysis of the Quaternary deposits for the assessment of the water logging problem of El Fayoum Depression. Ph.D. The-sis, Fac. Of Sci., Al-Azhr Univ., Egypt, 233.

Gad A, El-Zeiny A (2016) Spatial analysis for sustainable development of El Fayoum and Wadi El Natrun Desert Depressions, Egypt with the aid of remote sensing and GIS. Environ Earth Sci 8(3):1–18. https://doi.org/10.9734/JGEESI/2016/29706

Gad M, Dahab K, Ibrahim H (2018) Applying of a geochemical model on the Nubian sandstone aquifer in Siwa Oasis, Western Desert, Egypt. Environ Earth Sci 77:401–415. https://doi.org/10.1007/s12665-018-7580-6

Gad M, El-Hattab M (2019) Integration of water pollution indices and DRASTIC model for assessment of groundwater quality in El Fayoum Depression, western desert Egypt. J Afr Earth Sci 158:103554. https://doi.org/10.1016/j.jafrearsci.2019.103554

Gad M, Saad A (2017) Hydrogeochemical evaluation of fractured Limestone aquifer by applying a geochemical model in eastern Nile Valley, Egypt. Environ Earth Sci 76:641. https://doi.org/10.1007/s12665-017-6974-1

Garrels RM, Christ CL (1965) Solutions, minerals, and equilibria. Freeman, Dallas, p 450

Gibbs RJ (1970) Mechanisms controlling world water chemistry. Science. 170:10881

Giménez-Forcada E, San Román FJS (2015) An excel macro to plot the HFE-Diagram to identify seawater intrusion phases. Ground Water 53(5):819–824. https://doi.org/10.1111/gwat.12280

Hussein HA, Ricka A, Kuchovsky T, El Osta MM (2017) Groundwater hydrochemistry and origin in the south-eastern part of Wadi El Natrun, Egypt. Arab J Geosci 10:170–184. https://doi.org/10.1007/s12517-017-2960-x

Jalali M (2005) Nitrates leaching from agricultural land in Hamadan, western Iran. Agric Ecosyst Environ 110:210–218. https://doi.org/10.1016/j.agee.2005.04.011

Jalali M (2007) Hydrochemical identification of groundwater resources and their changes under the impacts of human activity in the Chah Basin in western Iran. Environ Monit Assess 130(1–3):347–367. https://doi.org/10.1007/s10661-006-9402-7

Joshi A, Seth G (2011) Hydrochemical profile for assessing the groundwater quality of Sambhar Lake City and its Adjoining area. Environ Monit Assess 174:547–554. https://doi.org/10.1007/s10661-010-1477-5

Kachroud M, Trolard F, Kefi M, Jebari S, Bourrié G (2019) Water quality indices: challenges and application limits in the literature. Water 11:361. https://doi.org/10.3390/w11020361

Kanagaraj G, Elango L, Sridhar SGD (2018) Hydrogeochemical processes and influence of seawater intrusion in coastal aquifers south of Chennai, Tamil Nadu, India. Environ Sci Pollut Res 1–23. https://doi.org/10.1007/s11356-017-0910-5

Kawoa NS, Karuppannanb S (2018) Groundwater quality assessment using water quality index and GIS technique in Modjo River Basin, central Ethiopia. J Afr Earth Sci 147:300–311. https://doi.org/10.1016/j.jafrearsci.2018.06.034

Khalil MTI, Fishar MR, Shakir SH, Amer AS, Nassif MG (2017) Impact of drainage water on macrobenthos structure of Lake Qaroun, El-Fayoum, Egypt. Egypt J Aquat Res 21(2):17–32

Khan MYA, Gani KM, Chakrapani GJ (2017) Spatial and temporal variations of physicochemical and heavy metal pollution in Ramganga River—a tributary of River Ganges, India. Environ Earth Sci 76:231–243. https://doi.org/10.1007/s12665-017-6547-3

Kumar SK, Logeshkumaran A, Magesh NS, Prince S, Godson N, Chandrasekar (2015) Hydro-geochemistry and application of water quality index (DWQI) for groundwater quality assessment, Anna Nagar, part of Chennai City, Tamil Nadu, India. Appl Water Sci 5:335–343. https://doi.org/10.1007/s13201-014-0196-4

Kumar V, Sharma A, Kumar R, Bhardwaj R, Thukral AK, Rodrigo-Comino J (2018) Assessment of heavy-metal pollution in three different Indian water bodies by combination of multivariate analysis and water pollution indices. Hum Ecol Risk Assess 26:1–16. https://doi.org/10.1080/10807039.2018.1497946

Li P, Tian R, Xue C, Wu J (2017) Progress, opportunities and key fields for groundwater quality research under the impacts of human

activities in China with a special focus on western China. Environ Sci Pollut Res 24(15):13224–13234. https://doi.org/10.1007/s11356-017-8753-7

Li P, He S, Yang N, Xiang G (2018) Groundwater quality assessment for domestic and agricultural purposes in Yan'an City, northwest China: implications to sustainable groundwater quality management on the Loess Plateau. Environ Earth Sci 77(23):775. https://doi.org/10.1007/s12665-2018-7968-3

Li P, He X, Li Y, Xiang G (2019a) Occurrence and health implication of fluoride in groundwater of loess aquifer in the Chinese Loess Plateau: a case study of Tongchuan, Northwest China. Expo Health 11(2):95–107. https://doi.org/10.1007/s12403-018-0278-x

Li P, Tian R, Liu R (2019b) Solute geochemistry and multivariate analysis of water quality in the GuohuaPhosphorite Mine, Guizhou Province, China. Expo Health 11(2):81–94. https://doi.org/10.1007/s12403-018-0277-y

Metwaly M, El-Qady G, Massoud U, El-Kenawy A, Matsushima J, Al-Arifi N (2010) Integrated geoelectrical survey for groundwater and shallow subsurface evaluation: case study at Siliyin spring, El-Fayoum, Egypt. Int J Earth Sci 99:1427–1436. https://doi.org/10.1007/s00531-009-0458-9

Mgbenu CN, Egbueri JC (2019) The hydrogeochemical signatures, quality indices and health risk assessment of water resources in Umunya district, southeast Nigeria. Appl Water Sci 9:22. https://doi.org/10.1007/s1320.1-019-0900-5

Mohamed EA, El-Kammar AM, Yehia MM, Abu Salem HS (2015) Hydrogeochemical evolution of inland lakes' water: a study of major element geochemistry in the Wadi El Raiyan Depression, Egypt. J Adv Res 6(6):1031–1044. https://doi.org/10.1016/j.jare.2014.12.008

Ndoye S, Fontaine C, Gaye CB, Razack M (2018) Groundwater quality and suitability for different uses in the Saloum Area of Senegal. Water 10:1837. https://doi.org/10.3390/w10121837

Piper AM (1944) A graphic procedure in the geochemical interpretation of water-analyses. EOS Trans Am Geophys Union 25(6):914–928. https://doi.org/10.1029/TR025i006p00914

Plummer LN, Parhurst DL, Fleming GW, Dunkel SA (1991) A computer program incorporating pitzers equations for calculation of geochemical reactions in brines. US Geological Survey. Water-Resources investigations report, 88–4153. https://doi.org/10.3133/wri884153

Rana R, Ganguly R, Gupta AK (2018) Indexing method for assessment of pollution potential of leachate from non-engineered landfill sites and its effect on groundwater quality. Environ Monit Assess 190(1):1–23. https://doi.org/10.1007/s10661-017-6417-1

Redwan M, Elhaddad E (2017) Heavy metals seasonal variability and distribution in Lake Qaroun sediments, El-Fayoum, Egypt. J Afr Earth Sci 134:48–55. https://doi.org/10.1016/j.jafrearsci.2017.06.005

Richards LA (1954) Diagnosis and improvement of saline and alkali soils. Hand Book, No. 60. U.S. Department of Agriculture, Washington

Schoeller H (1967) Geochemistry of groundwater. An international guide for research and practice. UNESCO 15:1–18

Sharma A, Ganguly R, Gupta AK (2020) Impact assessment of leachate pollution potential on groundwater: an indexing method. J Environ Eng 146(3):05019007. https://doi.org/10.1061/(ASCE)EE.1943-7870.0001647

Simsek C, Gunduz O (2007) IWQ index: a GIS-integrated technique to assess irrigation water quality. Environ Monit Assess 128:277–300. https://doi.org/10.1007/s10661-006-9312-8

Singarajam C, Chidambaram S, Srinivasamoorthy K, Anandhan P, Selvam S (2015) A study on assessment of credible sources of heavy metal pollution vulnerability in groundwater of Thoothukudi Districts, Tamilnadu, India. Water Qual Expo Health 7:459–467. https://doi.org/10.1007/s12403-015-0162-x

Subba Rao N, Chaudhary M (2019) Hydrogeochemical processes regulating the spatial distribution of groundwater contamination, using pollution index of groundwater (PIG) and hierarchical cluster analysis (HCA): a case study. Groundw Sustain Dev 9:100238. https://doi.org/10.1016/j.gsd.2019.100238

Tiwari TN, Manzoor A (1988) River pollution in Kathmandu valley (Nepal) suitability of river water for irrigation. Indian J Environ Prot 8(4):269–274

Tripaty JK, Sahu KC (2005) Seasonal hydrochemistry of groundwater in the Barrier Spit system of the Chilika Lagoon, India. J Environ Hydrol 13:1–9

WHO (2017) Guidelines for drinking water quality [electronic resource]: 4thedn. Geneva, pp 307–441. ISBN: 978 92 4 154815 1 (WEB version). http://whqli bdoc.who. int/publications/2011/97892 41548 151_eng.pdf

Wu J, Zhou H, He S, Zhang Y (2019) Comprehensive understanding of groundwater quality for domestic and agricultural purposes in terms of health risks in a coal mine area of the Ordos basin, north of the Chinese Loess Plateau. Environ Earth Sci 78(15):446. https://doi.org/10.1007/s12665-019-8471-1

Xiao J, Jin Z, Zhang F, Wang J (2012) Solute geochemistry and its sources of the groundwaters in the Qinghai Lake catchment, NW China. J Asian Earth Sci 52:21–30. https://doi.org/10.1016/j.jseaes.2012.02.006

Yang Q, Li Z, Ma H, Wang L, Martin JD (2016) Identification of the hydrogeochemical processes and assessment of groundwater quality using classic integrated geochemical methods in the Southeastern part of Ordos's basin, China. Environ Pollut 218:879–888. https://doi.org/10.1016/j.envpol.2016.08.017

Zhang X, Hu BX, Wang P, Chen J, Yang L, Xiao K (2018) Hydrogeochemical evolution and heavy metal contamination in groundwater of a reclaimed land on Zhoushan Island. Water 10(3):316–338. https://doi.org/10.3390/w10030316